AD_____

Award Number: W81XWH-10-1-0732

TITLE: Mass Scale Biosensor Threat Dianostic for In-Theater Defense Utilization

PRINCIPAL INVESTIGATOR: Dr. Joe Simpson

CONTRACTING ORGANIZATION: Florida International University
Miami, FL 33174

REPORT DATE: October 2011

TYPE OF REPORT: Annual

PREPARED FOR: U.S. Army Medical Research and Materiel Command
Fort Detrick, Maryland 21702-5012

DISTRIBUTION STATEMENT: Approved for public release; distribution unlimited

REPORT DOCUMENTATION PAGE

Form Approved
OMB No. 0704-0188

1. REPORT DATE *(DD-MM-YYYY)*	2. REPORT TYPE	3. DATES COVERED *(From - To)*
01-10-2011	Annual	20 Sep 2010 - 19 Sep 2011

4. TITLE AND SUBTITLE
Mass Scale Biosensor Threat Dianostic for In-Theater Defense Utilization

5a. CONTRACT NUMBER

5b. GRANT NUMBER
W81XWH-10-1-0732

5c. PROGRAM ELEMENT NUMBER

6. AUTHOR(S)
Dr. Joe Simpson

E-Mail: simpsonj@fiu.edu

5d. PROJECT NUMBER

5e. TASK NUMBER

5f. WORK UNIT NUMBER

7. PERFORMING ORGANIZATION NAME(S) AND ADDRESS(ES)
Florida International University
Miami, FL 33174

8. PERFORMING ORGANIZATION REPORT NUMBER

9. SPONSORING / MONITORING AGENCY NAME(S) AND ADDRESS(ES)
U.S. Army Medical Research and Materiel Command
Fort Detrick, Maryland 21702-5012

10. SPONSOR/MONITOR'S ACRONYM(S)

11. SPONSOR/MONITOR'S REPORT NUMBER(S)

12. DISTRIBUTION / AVAILABILITY STATEMENT
Approved for Public Release; Distribution Unlimited

13. SUPPLEMENTARY NOTES

14. ABSTRACT

The goals of this project are to develop two biosensors capable of rapidly assessing exposure to unknown toxicants and to validate these biosensors by "gold-standard" cytogenetic assays. We have made significant progress in all three areas of the project. IRB documentation has been completed and 9 subjects recruited for blood draws. H2O2 has been demonstrated to increase the frequency and severity of chromosome aberrations with increasing concentrations. Two biosensors have been developed. For the EIST biomarker we demonstrated the feasibility of detecting the 8-OHdG biomarker using a disposable paper-based strip and screen printed electrodes, which provides the fundamental underpinning for integration of electrodes to paper strips for quantitative measurements of 8-OHdG. For the gold nanoparticle whole-cell based biosensor, we have completed dose and time kinetics studies to quantify the expressed stress proteins –Hsp70 and Rad54, in response to environmental stress H2O2 and UV using ELISA. We have successfully measured standard forms of Caspase-3, RAD54 and Hsp70 using the 3-D Silver colloidal nanosphere as SERS substrate and demonstrated that Caspase-3 can be measured to 1 ng/ml (below the level of detection by commercial ELISA kits-4.8 ng/ml). During the next year we will assess the accuracy and reliability of these 2 biosensors

15. SUBJECT TERMS
Biosensors to detect exposure to unspecified toxicants Validation of cytogenetic gold standard assays
Gold nanoparticles and Raman spectroscopy Reactive oxidative DNA damage and 8-OHdeoxyguanosine

16. SECURITY CLASSIFICATION OF:			17. LIMITATION OF ABSTRACT	18. NUMBER OF PAGES	19a. NAME OF RESPONSIBLE PERSON
a. REPORT	b. ABSTRACT	c. THIS PAGE			USAMRMC
U	U	U	UU	40	19b. TELEPHONE NUMBER *(include area code)*

Table of Contents

1. General Introduction

Currently there is no practical or rapid method to monitor exposures to biological weapons of unknown nature, either chemicals or pathogens on the battlefield or chemicals encountered during environmental cleanup programs. Need is especially acute for assessing exposures to unspecified toxicants, i.e., agents unknown at time of exposure. If the toxic agent were known, a specific assay could be readily developed, and indeed many options already exist to detect specific toxicants. If the toxic agent is not known or suspected, a different approach is necessary to monitor the exposure to toxicity. Inexpensive assays must be developed that provide rapid assessment and warn of toxicity in the environment (e.g., in water and air) and personnel exposure. This could then be followed by more detailed and expensive laboratory analysis to identify the specific toxicant. Sorely needed is a device comparable to the familiar dosimeter "badge", which determines cumulative radiation exposures. The current approach for assessing radiation and genome toxicity relies principally on scoring for chromosomal abnormalities. These measures of genotoxicity are currently only possible through laborious cytogenetic evaluations requiring dedicated lab personnel with extensive training.

No biomedical devices can identify exposures to toxicants sensitively and in "real-time" fashion. Thus, at the present time, cytogenetic methods remain the "gold-standard", but "rapid" user-friendly (i.e., less labor intensive) and cost-effective methods are desired. The goals of this project are to develop two biosensors (i) EIST biosensor measuring reactive oxygen species specifically 8-OHdG; and (ii) SERS biosensor measuring several stress proteins. Each should be capable of rapidly assessing exposure to toxicants that are unknown or unspecified and validated by proven cytogenetic assays.

1.1. Gold-Standard Cytogenetic Assays Background

Assessments of the effects of chemical and physical agents on DNA have been made using a variety of genotoxicity and mutagenicity assays. Unfortunately, the numerous mechanisms through which different genotoxic agents can act dictate that no single test can detect all forms of DNA damage. Testing requires a multifaceted approach. Standard cytogenetic assays used for comparison in this project represent the "industry gold-standard" assays for genotoxicity and biomonitoring testing: Chromosome Aberration assay (CA); Micronuclei assay (MN); and Comet assays.

Clastogenic and aneugenic agents have been shown to result in a biologically significant increase in the frequency of cells with structural or numerical chromosomal aberrations. The CA assay detects both numerical and structural aberrations. The MN assay counts small extranuclear bodies that are formed during mitosis as a result of chromosome breaks or interference in the mitotic process, resulting in lagging chromosome(s) that lead to formation of MN (Sari-Minodier et al., 2007). The Comet assay measures DNA damage resulting from single- and double-stranded breaks. Undamaged DNA retains its highly organized association with matrix proteins in the nucleus. When damaged, however, this organization is disrupted; DNA fragments disperse and migrate out of the cell nuclei (Glei et al., 2009).

To increase sensitivity, CA, MN, and Comet assays will be combined with fluorescent *in-situ* hybridization (FISH) to evaluate sensitivity and specificity vis a vis the two biosensors being developed. FISH is a commonly used cytogenetic method in which fluorescent probes target and fluorescently "paint" chromosomal regions of interest.

1.2. Biosensor 1 Background: EIST Based Biomarker Sensor For Oxidative DNA Damage Assessment

Numerous agents of biological and chemical warfare (Kang et al., 2006 Kuhn et al., 2006) induce oxidative damage in cells. 8-OHdG is the most commonly studied biomarker for cellular oxidative stress, DNA damage and repair mechanisms. Upon oxidation, a hydroxyl free radical attack arises at the C-8 position of deoxyguanosine in DNA, resulting in production of 8-Hydroxy-2-deoxyguanosine (8-OHdG) (Kasai et al., 1984). Urinary 8-OHdG is commonly measured in the laboratory setting; elevated urinary 8-OHdG concentrations are associated with environmental exposures including chemical toxins (Erhola et al., 1997) and radiation (Sperati et al., 1999). Levels of 8-OHdG are expected to be proportional to the cumulative toxicity levels of many toxicants and their duration of exposure. Periodic monitoring of 8-OHdG levels in personnel working at military installations and battlefield sites could thus enable assessment of unspecified toxicant exposure to various biological, chemical and radiation warfare agents. Here we will develop a simple competitive colloidal gold-based electrochemical immunoassay in lateral-flow format for the rapid detection of 8-OHdG. Nitrocellulose membrane strip is separately coated with goat anti-mouse IgG (control line) and 8-hydroxyguanosine-BSA conjugate (test line) (Figure 1). Initially anti-8-Hydroxyguanosine (8-OHG) monoclonal is labeled with Gold Nanoparticles. Using both standards and spiked urine solutions, a positive reaction results in the remaining antibody-gold conjugate combining with antigen coated on the membrane for obvious visual detection. Further, electrochemical capacity will be integrated into the same system to give better quantitative information. The test strip will thus provide a point-of-care testing method for quantitative, semi-quantitative, or qualitative detection of DNA oxidative stress with high sensitivity, specificity, speed of performance and the advantages of simplicity.

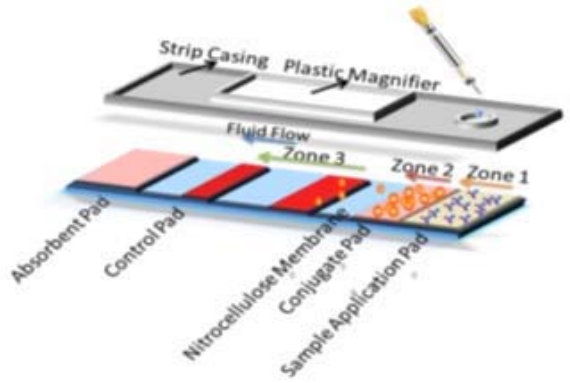

Figure 1. Schematic illustration of the lateral flow strip for 8-OHdG biomarker detection. Upon competitive type assays, the Au particles labeled by anti-8-OHdG antibody flow along a thin solid matrix together with the analytes driven by capillary force and eventually accumulate upon immune recognition at a defined area pretreated by antibody or antigen. Qualitative or semi-quantitative detection of various analytes is thus realized by colorimetry read either by naked eyes or with the aid of optical density analysis.

1.3. Biosensor 2 Background: SERS Based Gold Nanoparticle Whole-Cell Biosensor

Raman spectroscopy is used to identify chemical structures based on the inelastic scattering of light by the vibrational modes of chemical bonds of molecules. Scattering of a laser light from a protein produces a spectrum of Raman peaks, each characteristic of a specific vibration of a molecular bond. However, one of the primary limitations of Raman spectroscopy is its relatively low molecular cross-section (Aroca, 2006). Surface Enhanced Raman Spectroscopy (SERS) overcomes this limitation because localized electromagnetic enhancement in the order of $10^{11\text{-}14}$ occurs when the metal surface plasmons are excited in resonance with the laser radiation (Nie et al., 1997). For this reason, metal nanoparticles such as silver, gold, copper, and platinum are finding large applications in chemical and biological sensing.

Response of yeast to stress is well known (Magar et al., 1993). Utilizing yeast cells as a surrogate for the whole cell sensor development have several advantages: (i) they are eukaryotic and robust; (ii) able to be dried at 28-40^{o}C, stored for more than a year, and immobilized in various substrate including membranes and gel until needed. The robust living yeast cells can be used to monitor the exposure to environmental stress by developing a method to quantify the response (expression of proteins) of yeast to stress. The yeast serve as a surrogate for personal exposure.

The potential for label-free detection and identification of proteins by SERS, even intracellular proteins, has been well documented (Li et al., 2006). Specific proteins in cellular matrices and the intracellular environment can be detected based on a protein-protein (antibody-antigen) interaction using SERS. In this aspect, Gold Nanoparticles with optimal size around 30 nm have been utilized to detect proteins interactions. Combined with the aptitude for qualitative assessment, quantitative measurement ability using SERS to detect a wide range of molecules simultaneously makes SERS sensors versatile.

To measure the expressed stress proteins (Hsp70, Rad54 and Caspase-3), antibody-tagged Gold nanoparticles will be delivered into yeast cells followed by measurement of yeast response to stress such as UV, H_2O_2 and others non-invasively, using SERS. The sensor development will involve aspects of Gold Nanoparticle synthesis, linker attachment, antibody binding (Figure 2), nanoparticle uptake and detection of proteins both outside and within yeast cells, device fabrication and determination of the sensitivity in the measurement of stress proteins using existing conventional technique (ELISA or Western-blot).

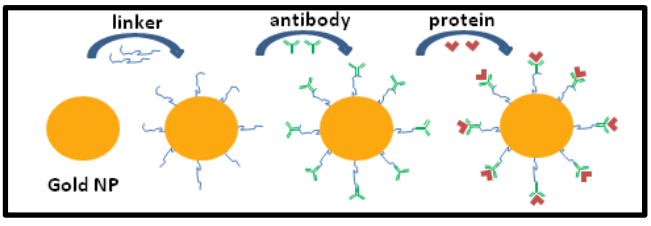

Figure 2. Schematic diagram of the Gold Nanoparticle SERS sensor. Presence of the protein conjugated to Gold Nanoparticle-antibody complex will be detectable by SERS.

2. Body

2.1. Cytogenetic Assays

OVERALL PROJECT OBJECTIVES: To establish and validate "gold-standard" cytogenetic assays CA, MN and the Comet assay, using standardized genotoxic agents H_2O_2 and UV to measure DNA damage in human lymphocytes in-vitro.

2.1.1. IRB Approval

The cytogenetics component of the "mass scale biosensor threat diagnostic for in-theater defense utilization" project required approval by both Florida International University (FIU) and the Telemedicine and Advanced Technology Research Center [TATRC] institutional review boards (IRB). IRB approval was essential prior to any commencement of laboratory work, because all assays outlined in the proposal (CA; MN and comet) require collection of human lymphocytes from healthy volunteers. In brief, the IRB proposal detailed the following: Healthy volunteers wishing to participate in this research study donate approximately 10ml of blood to be collected by venipuncture at the FIU University Health Center. Donors must be aged 18 to 70-years-old and required to complete a short lifestyle questionnaire determining any prior genotoxic exposure. Donors may be excluded from participating if they are deemed "unhealthy" on the basis of their responses on the questionnaire. Blood samples are de-identified and coded with a project number. Multiple blood cultures are established from blood collected from the research participants. These are cultured (in-vitro) in the presence of genotoxic agents (ultra-violet [UV] light and hydrogen peroxide [H_2O_2]). UV and H_2O_2 have been selected as genotoxic agents in this project since both have well defined mechanisms of action and are frequently utilized as positive controls "standardized" agents in DNA damage assays. Blood samples are cultured in the presence of these agents at increasing concentrations to establish a dose-effect relationship. The IRB proposal was initially submitted to the FIU IRB on the 11/10/2010 and approved to be sent to TATRC on the 12/10/2010. We received a request from TATRC to make some minor modifications, to which we adhered. The amended IRB proposal was sent to the FIU and then to TATRC IRBs. Final approval to commence recruiting research participants was given on 3/28/2011.

2.1.2. Research Participant Recruitment

In conjunction with the FIU University Health Center, guidelines were established at the outset of the project along with a standard operating protocol that was submitted as part of the supporting documents for the IRB process. Upon final approval of the project by the FIU and TATRC IRBs these were immediately instituted and are now fully operational. To date, we have recruited nine healthy participants (three male and six female) to donate blood for this project. No difficulty has been encountered in recruiting volunteers.

2.1.3. Blood Cultures

In order to be able to perform the CA, MN and Comet assays, human lymphocytes collected by venipuncture must be cultured and stimulated to enter cell division. The reason for this is twofold. First, the CA assay requires cells to be in a specific stage of cell division (metaphase) in order that the DNA is condensed, thus allowing identification of individual chromosomes based on size, centromere position and banding pattern after staining. Second, mammalian cells have a battery of repair mechanisms in their arsenal to correct DNA damage. This can be accomplished at various points as cells progress through the cell cycle. The end result of the induction of DNA damage and the various repair mechanisms available includes: (i) DNA damage can be repaired, resulting in DNA that is no longer altered; (ii) the cell is damaged beyond repair and initiates apoptosis (cell death). Apoptosis is initiated when a cell is unable to proceed past various cell cycle checkpoints, largely in place to recognize the presence of multiple/harmful unrepaired DNA damage; (iii) DNA damage is unsuccessfully recognized and/or repaired, but the cell evades apoptosis and manages to progress through the cell cycle. For the purposes of this project we are largely interested in points ii) and iii), primarily because the scenario listed in i) indicates that the DNA damage is minimal and passes unrecognized within the cell. Pathways ii) and iii) are clearly detrimental, apoptosis of large numbers of cells due to excessive DNA damage being potentially disastrous. Of more concern is DNA damage capable of evading DNA damage recognition and/or repair persisting in the cell such that future generations of the cell continue to divide. In this situation the DNA damage can be passed to future daughter cells, and depending on the type of damage and location within the genome, could result in diseases such as cancer. Therefore, we have focused our attention on exposing lymphocytes to genotoxic agents in-vitro but allowing cells to divide in culture. We can thus analyze DNA damage that has evaded DNA repair mechanisms and cell cycle check points to persist.

Our laboratory has established the requisite parameters to optimize the culturing of human lymphocytes. These are largely the same for all three DNA damage assays (CA, MN and Comet). Specifically, we have performed experiments to determine the culture conditions, appropriate culture media and various chromosome preparation methods to obtain a high yield of cell division and high quality metaphases for the CA assay. As per standardized guidelines for genotoxic assays, the mitotic index for each culture must be monitored. This measure of the proliferation status of a cell population is defined as the ratio between the number of cells in mitosis and the total number of cells. The maximum concentration of a genotoxic agent must not surpass a reduction of more than 50% cell proliferation compared to unexposed cell cultures (indicative of excessive amounts of DNA damage).

2.1.4. Dose-Responses

We are in the process of finalizing the range-finding experiments for in-vitro H_2O_2 exposure in blood cultures. To date, we have tested concentrations of H_2O_2 in the range of 0-200μmol/ml; this range was

chosen initially based on pre-existing published data that have traditionally utilized H_2O_2 as a positive control in various genotoxic assays. Initially, blood is drawn into lithium-heparin tubes to prevent clotting, and then aliquoted (500µl) into tubes with 9.5ml of RPMI culture media (Invitrogen, USA) to which the H_2O_2 is added to the desired final concentration (range 25µmol/ml- 200µmol/ml). Blood cultures are set up in duplicate or triplicate depending on the DNA damage assay. The lymphocytes are incubated with RPMI in the presence of H_2O_2 for 30 mins, after which the lymphocytes are spun down and the RPMI media containing the H_2O_2 is removed and replaced with PB Karyomax media containing phytohaemagglutinin to stimulate cell division (Invitrogen, USA). The PB Karyomax media does not contain the genotoxic agent H_2O_2, allowing DNA repair mechanisms and cell cycle checkpoints to be initiated. Lymphocytes are then cultured for 72 hrs. to allow repair of DNA damage, apoptosis and progression of cell division (with or without DNA damage). At 71 hrs, colcemid is added to the cultures, thus disrupting the microtubule formation necessary for cells to proceed through metaphase and complete their cell cycle. Colcemid is added to arrest those cells in metaphase ensuring we have a population of cells at the desired stage of the cell cycle (metaphase) for the CA assay. Lymphocytes are subsequently centrifuged, separated from the culture media and processed through hypotonic and fixation steps.

2.1.5. Chromosome Aberration Assay

Processed lymphocyte cultures as outlined above are placed on glass slides. Their mitotic index is calculated for the control (unexposed) and for each exposure concentration of the genotoxic agent H_2O_2 (0, 25, 100 and 200µmol/ml) (Table 1); each sample is replicated.

Table 1:	H_2O_2 concentration		
	25µmol/ml	100µmol/ml	200µmol/ml
Average % reduction in mitotic index (cell proliferation) compared to unexposed lymphocyte cultures	8%	22%	40%

Slides are subsequently stained with 4',6-diamidino-2-phenylindole (DAPI) to permit analysis of chromosomes for the CA assay, using reverse DAPI banding. Metaphase spreads are visualized and captured using an Olympus BX61 fluorescence microscope at a magnification of x1000 with Smart Capture image analysis software (Digital Scientific, UK). Captured images are then imported into the karyotyping software SmartType (Digital Scientific, UK), which enables the operator to isolate individual chromosomes and classify each chromosome on the basis of size, centromere position and banding pattern (Figure 3).

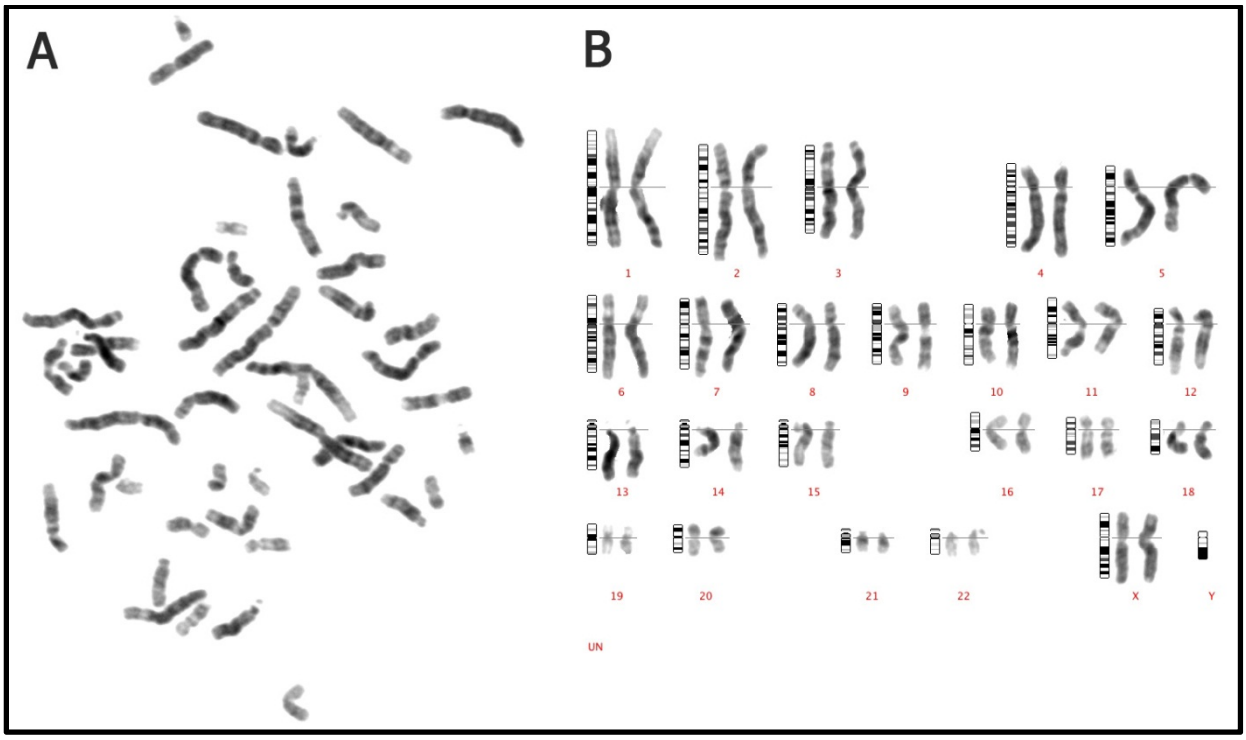

Figure 3: A) Reverse DAPI banded chromosome metaphase spread, illustrating how chromosomes can be visualized after staining with DAPI and identified by characteristic banding patterns, chromosome size and centromere position. B) A normal 46,XX female karyotype. This demonstrates how chromosomes (taken from Figure 1A) can be isolated, identified and aligned. G-band ideograms (schematic representation of the banding patterns) are located to the left of each chromosome pair. Chromosome number is indicated beneath the respective chromosome pairs.

A minimum of 50 metaphases are analyzed per sample per concentration of genotoxic agent (e.g., 0, 25, 100 and 200µmol/ml) of $H_2O_{2)}$ in duplicate; therefore, 100 metaphases are analyzed per sample per concentration.

To date, our analysis of cultured lymphocytes from individuals not exposed to any genotoxic agent (all nine study participants) showed a normal human karyotype (normal chromosomes). Five (5) subjects had lymphocytes cultured in the presence of the genotoxic agent H_2O_2. Lymphocytes from these subjects showed chromosome aberrations deemed by the CA assay to be the result of exposure to the genotoxic agent H_2O_2.

The CA assay enables identification of chromosomal aberrations (e.g., deletions, duplications, translocations, fragile sites and inversions) that are at least 5 megabases (Mb) in size. Specific observations include a reduction in cell proliferation (Table 1) and an increase in cell lysis with increasing H_2O_2 concentration. In addition, we have been able to observe abnormalities at all concentrations tested (25, 100 and 200µmol/ml), their frequency and severity increasing with higher concentrations (Figures 4-8).

At lower concentration (25µmol/ml H_2O_2), we find chromosomal breakages (Figure 4) and chromosomal fragile sites (Figure 5), which often appear as non-staining chromosome gaps that are frequently accompanied by DNA strand breakage (Glover et al., 1988). At higher H_2O_2 concentrations (100µmol/ml and 200µmol/ml) we have observed multiple defects including large terminal chromosome deletions, which involve loss of material at the ends of chromosomes (Figure 6). We also identified a number of metaphases with premature centromere separation (Figure 7), whereby centromeres prematurely separate in metaphase versus anaphase. This can lead to altered spindle checkpoint activation and impaired cell proliferation (Gordillo et al., 2009). Premature centromere separation is frequently also observed with premature sister-chromatid separation (Figure 7), in which cohesion of sister-chromatids is aberrant. This situation can be associated with chromosome aneuploidy (gain or loss of one or more chromosome(s) from the normal diploid number). With the highest tested H_2O_2 concentration (200µmol/ml), approximately 5-10% of metaphase spreads were not analyzable. In these cases the morphology of the chromosomes was altered, specifically chromosome size, centromere position and banding morphology (Figure 8). This phenomenon was observed only at the highest concentration of H_2O_2 (200µmol/ml).

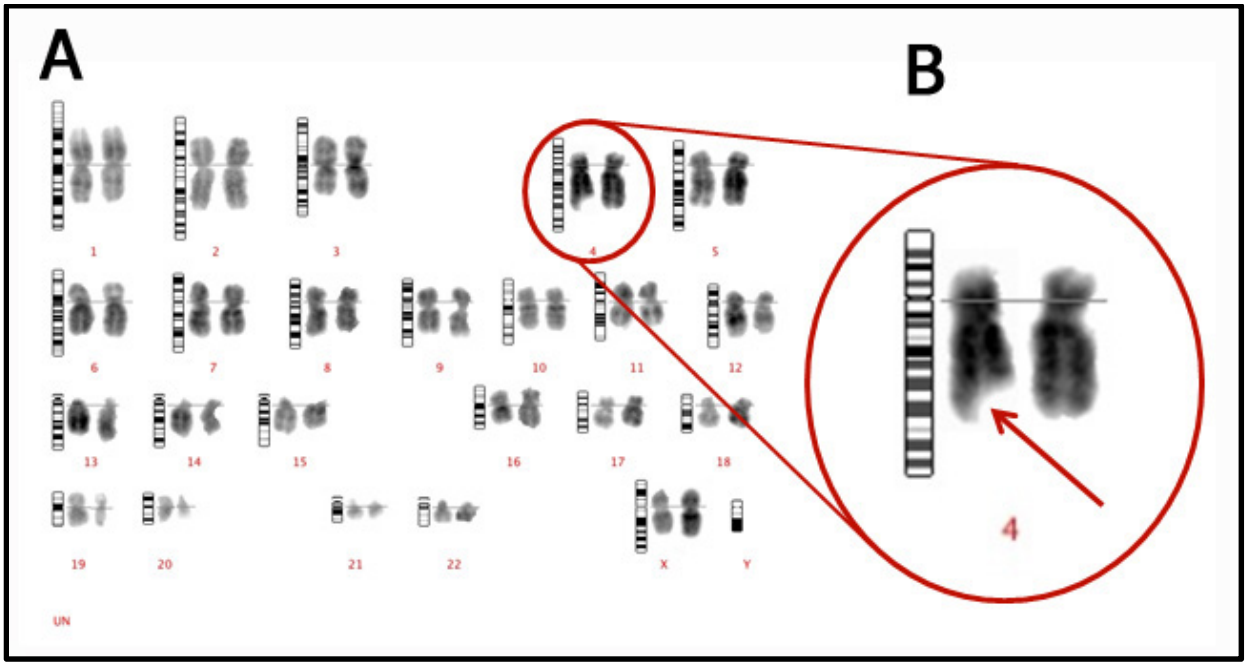

Figure 4: Reverse DAPI banding of a human metaphase (karyotype) obtained after incubation for 30 minutes with 25µmol/ml H_2O_2, followed by 72 hours of culture, cell fixation with hypotonic treatment and DAPI staining. A) The karyotype obtained shows 46 chromosomes and two X chromosomes and is therefore normal chromosome number. B) Enlargement of chromosome 4 illustrates a chromosomal breakage (arrow) in which a segment of the end of a chromatid has been lost.

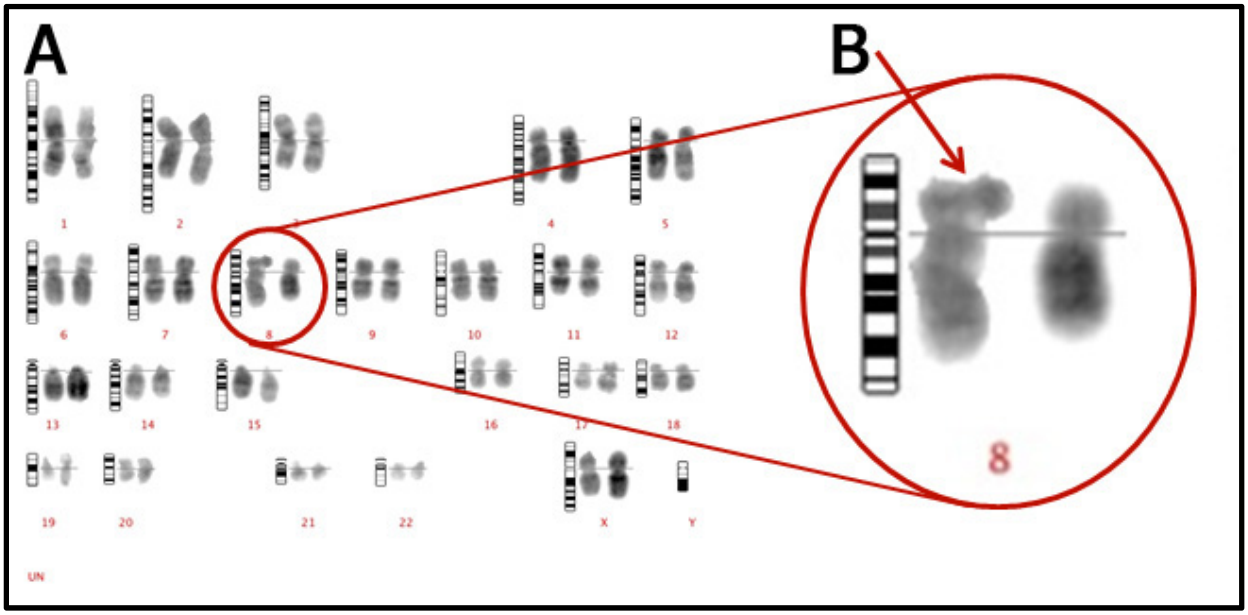

Figure 5: Reverse DAPI banding of a human metaphase (karyotype) obtained after incubation for 30 minutes with 25µmol/ml H_2O_2, followed by 72 hours of culture, cell fixation hypotonic treatment and DAPI staining. A) The karyotype obtained which shows 46 chromosomes and two X chromosomes and therefore normal chromosome number. B) Enlargement of chromosome 8 illustrates a fragile site (arrow) likely the result of DNA breakage.

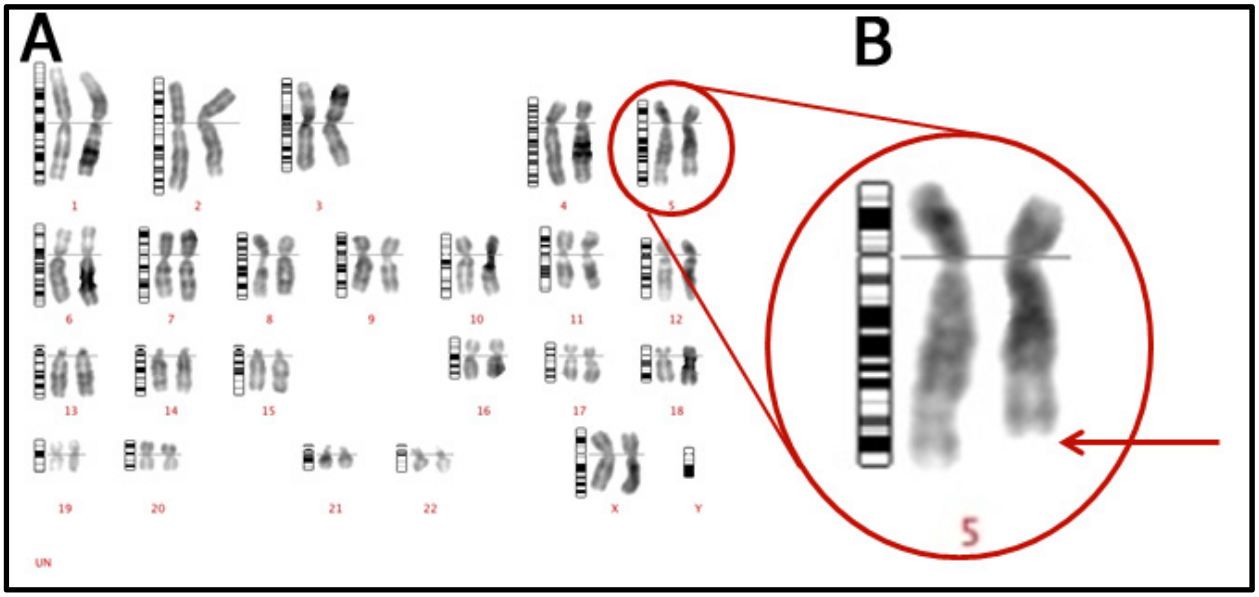

Figure 6: Reverse DAPI banding of a human metaphase spread obtained after incubation for 30 minutes with 100µmol/ml H_2O_2, followed by 72 hours of culture, cell fixation with hypotonic treatment and DAPI staining. A) The karyotype obtained shows 46 chromosomes and two X chromosomes and therefore normal in chromosome number. B) However, enlargement of chromosome 5 illustrates a large terminal deletion (arrow) in which a segment of the end of the chromosome has been lost.

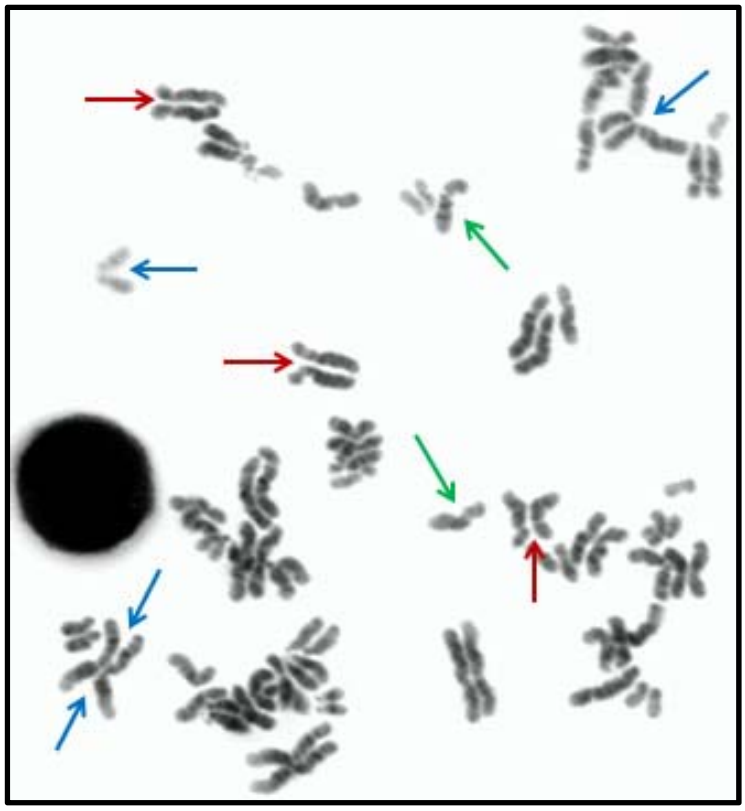

Figure 7: Reverse DAPI banding of a human metaphase spread obtained after incubation for 30 minutes with 200µl/ml H_2O_2, followed by 72 hours of culture, cell fixation hypotonic treatment and DAPI staining. Metaphase spread demonstrates normal chromosomes (green arrows); premature sister-chromatid separation, where the centromeres are still joined (blue arrows) and premature centromere separation, where there appears to be no connection between centromeres (red arrows).

Figure 8: Reverse DAPI banding of a human metaphase obtained after incubation for 30 minutes with 200µmol/ml H_2O_2, followed by 72 hours of culture, cell fixation with hypotonic treatment and DAPI staining. Observed are multiple chromosomes (some indicated by arrows) demonstrating altered morphology, with a wavy or bent morphology (not usually observed). Lack of relatively straight chromosomes makes determining size difficult. The banding pattern is often indistinct, with fairly homogenous dark segments extending across very large segments of the chromosome or entire chromosomes. In addition, the location of the centromere (site of the primary constriction) is often difficult to identify, these centromeric regions appearing "puffy". These factors in combination make it impossible to identify the vast majority of the chromosomes in this metaphase spread.

2.1.6. Fluorescence In-Situ Hybridization (FISH)

Fluorescence in-situ hybridization (FISH) allows identification of specific regions of interest in the genome by "fluorescently painting". In brief, the methodology involves DNA probes that can be manufactured in the lab or purchased and correspond to specific regions of the genome (e.g., a single whole chromosome; a small region specific to a certain chromosome such as a gene, centromere or telomere) (Figure 9). These probes can be applied to metaphase chromosomes and interphase nuclei to highlight or "paint" specific regions of interest.

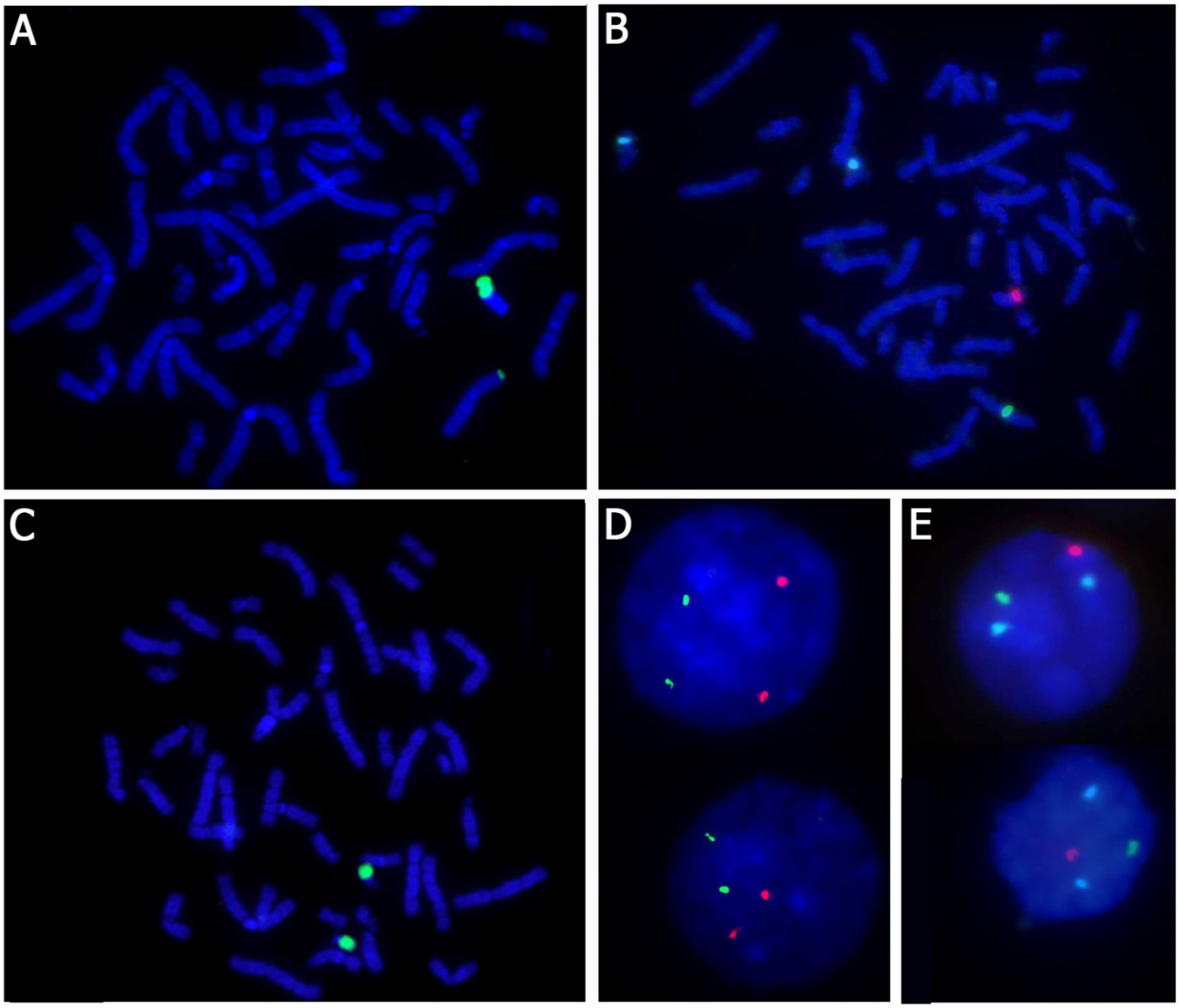

Figure 9: Fluorescent in-situ hybridization images A-E. DNA (interphase nuclei and metaphase chromosomes) is stained with DAPI (blue). A) FISH utilizing whole chromosome paint for chromosome Y (green) on a human metaphase. B) FISH using centromeric probes for chromosome 18 (aqua), chromosome Y (red) and chromosome X (green) on a human metaphase. C) FISH utilizing a whole chromosome paint for chromosome 22 (green) on a human metaphase. D) FISH using locus specific probes for chromosomes 13 (green) and 21 (red) in human lymphocyte nuclei. E) FISH using centromeric probes for chromosome 18 (aqua), chromosome Y (red) and chromosome X (green) in human lymphocyte nuclei.

By denaturing lymphocyte cells or chromosomes target DNA becomes single stranded, potentially enabling a FISH probe to hybridize to its homologous sequence if present in the cell or the chromosome. Hybridization overnight, followed by post-hybridization washes the following day, this allows target DNA to renature with the fluorescent probes incorporated within the target DNA. The target DNA and fluorescent probes are then visualized, captured and analyzed using fluorescent microscopy with associated capture software.

FISH can now be combined with the three DNA damage assays, but prior to this it is essential to establish the experimental parameters for optimal FISH results. We have thus tested a variety of commercially available probes in various target cells (nuclei and chromosomes). These include centromeres, locus specific probes and whole chromosome paints in both interphase nuclei and metaphase chromosomes (Figure 9). We have established the optimum parameters, specifically: pre-treatment of the target material; hybridization temperature, hybridization duration and post-hybridization washes for each of these probe types.

2.2. EIST Based Biomarker Sensor For Oxidative DNA Damage Assessment

OVERALL OBJECTIVES: The overall goal of this stage of the project (2010-2012) is to develop a paper-based biosensor which integrates the immunochromatography method and electrochemical method for qualitative and quantitative detection of the DNA oxidative damage biomarker-8 hydroxy-2-deoxy-guanosine (8-OHdG). Human urine samples will be used to assess toxic exposure assessment.

2.2.1. Material Preparations: Functional Gold Nanoparticles Preparation And Lateral Flow Strips Fabrication

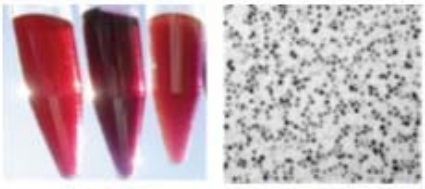

Figure 10. Left: Synthesized gold nanoparticles in different sizes from 2 nm to 100 nm. Right: SEM characterization of gold nanoparticles.

- **Synthesized And Characterized Gold Nanospheres**

Synthesized gold nanospheres are used as signaling reporters in immuno paper strips. We thus synthesized gold nanoparticles with sizes ranging from 5- 100 nanometers. Particle size, and surface charge properties have been characterized by SEM and Malvern particle size analyzer (Figure 10).

- **Conjugation Of Antibody To The Gold Nanoparticles**

Antibody-functionalized Gold Nanoparticles are used for the conjugation pad of the lateral flow strips. Specificity of the lateral flow strips relies on the conjugation pad. A series of experiments was conducted, varying the ratio of antibody and Gold Nanoparticles. The optimized condition of antibody-conjugating Gold Nanoparticles was thus established.

- **Paper Strip Fabrication**

In general, there are two types of lateral flow strips: direct solid-phase (also called sandwich) immunoassay and competitive solid-phase immunoassay. Choice depends on the molecular sizes and the immunological properties of targeting molecules (Ngom et al. 2010). Typically, direct type strips are used when testing for larger analytes, which have multiple antigenic sites. Because the analytes have multiple antigenic sites, the sandwich approach is used, the testing line normally modified by a secondary antibody to capture the conjugation of analyte-Gold Nanoparticles. Competitive formats are typically used when testing for small molecules having single antigenic determinants, which cannot bind to two antibodies simultaneously. The analytes pre-immobilized on the test line will competitively bind to the conjugation of antibody-Gold Nanoparticle against the analyte in the samples. We have fabricated and tested the two types of lateral flow strips (Figure 11) using biomolecules in different sizes including whole bacterial cells (big size) and DNA damage biomarker 8-OHdG (small size) to understand the effects of the molecule sizes on the immunoassay. We demonstrate that 8-OHdG has only a single antigenic site; therefore, the competitive mode is more applicable for 8-OHdG detection than the sandwich-type detection mechanism. In addition, the competitive mode shows good relation between color intensity on the testing line and concentration of 8-OHdG analyte, indicating capability of semi quantitative analysis of 8-OHdG using the lateral strip. The 8-OHdG analyte was also electrochemically measured using different type of screen-printed electrode, which provided better quantitative information of 8-OHdG concentration. In the future, we plan to integrate the two detection platforms, including screen-printed electrode and paper-based lateral flow strip, to develop an easy-to-use, disposable and reliable sensing platforms for 8-OHdG measurements.

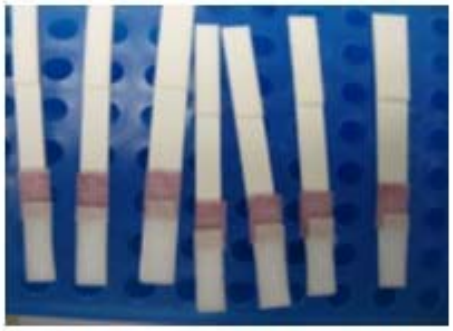

Figure 11. The fabricated lateral flow immuno strips before running analyte samples.

2.2.2. Testing Immuno Lateral Strips Based On Direct Solid-Phase (Sandwich) Immunoassay

Achievement 1. We first fabricated and tested the sandwich-type lateral strips to understand the immuno properties in term of the number of antigenic sites of 8-OHdG. We used bacterial cells, which have multiple antigenic sites, as control samples to demonstrate the capability of the sandwich-type lateral flow strips. For 8-OHdG detection, we found that the sandwich-type lateral strip was capable of measuring 8-OHdG only in micro molar concentration level, indicating the sensitivity of the strip is too low to be used for 8-OHdG detection in the range of biological concentrations (Figure 12). In addition, we could not obtain data showing the

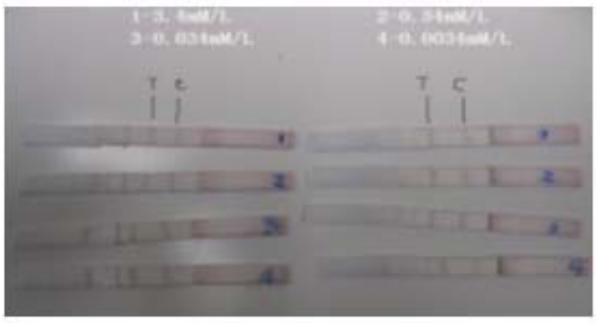

Figure 12. Measurement of 8-OHdG using the lateral flow strips based on sandwich immunoassay mechanism. T are the testing lines showing the detection of 8-OHdG. No significant color difference at the test lines are observed using different concentrations of 8-OHdG.

expected correlation of the color intensity of test line to the concentrations of 8-OHdG. This result demonstrated that 8-OHdG has a single antigenic determinant and, hence, not applicable for the "sandwich" detection mode. We conclude here that the competitive type design will be more suitable for 8-OhdG detection than the sandwich-type strips, which have shown no detection of 8-OHdG in micro molar concentrations.

Achievement 2. Using the sandwich-type strips, we successfully detected pathogen bacterial cells. Color intensities of the testing line are proportional to the concentration of bacterial cells (Figure 13). We demonstrated that the sandwich-detecting mechanism is suitable for the detection of biomolecules which have multiple immuno antigenic determinants, but not for single antigenic site molecule like 8-OHdG. Detection range of the bacteria lies within 500-5000 CFU/ml. **Our results led to one peer reviewed journal publication (Li et al., Paper based point-of-care testing disc for multiplex whole cell bacteria analysis, Biosensors and Bioelectronics 26:4342, 2011).**

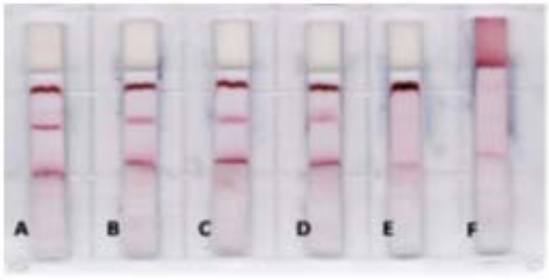

Figure 13. Preliminary testing of sandwich type immnosensor strip to establish the proof of concept. Samples, A) $5x10^3$ CFU/ml B) $4x10^3$ CFU/ml C) $3x10^3$ CFU/ml D) $0.5x10^3$ CFU/ml of S. aureus E) Buffer (control with no pathogens) F) $5x10^3$ CFU/ml of S. aureus bacterial cells.

2.2.3. Testing Immuno-Lateral Strips Based On Competitive Mode

Different from the "sandwich" detection mechanism, the competitive mode mechanism is based on competitive binding of anti-8-OHdG antibody to the 8-OHdG contained in samples and in the test line. In this mode, the 8-OHdG itself rather than the secondary antibody is immobilized on the test line.

- **Immobilization of 8-OHdG**

To prevent the egress of 8-OHdG due to the liquid flow on the strip, Bovine Serum Albumin (BSA) conjugated 8-OHdG was synthesized and used to modify the test line. We found immobilization of 8-OHdG via BSA conjugation is very stable and reproducible.

- **Detection Of 8-OHdG Using The Competitive Mode-Based Lateral Flow Strips**

We successfully detected 8-OHdG in standard buffer solution with a detection limit 100 pg/ml. In addition, the calibration curve in Figure 14 indicates the color intensity at test lines decreases gradually with increasing concentrations of 8-OHdG

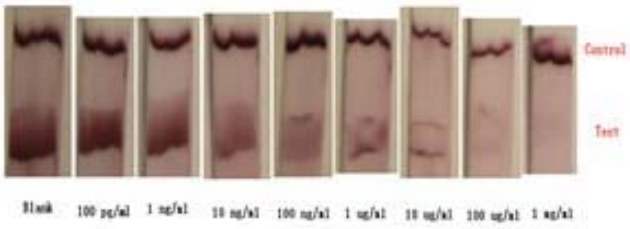

Figure 14. Color intensity on strips at 6 mins, from blank to 1.0 mg/ml. From left to right, the color intensities on testing lines gradually decreased with increasing the concentration of 8-OHdG. The detection limit is 100 pg/ml.

from 100 pg/ml to 1.0 mg/ml. Color intensities are relatively proportional to the concentrations of analyte. (Figure 15) Color is not observed at control line when the 8-OHdG concentration is higher than 1.0 mg/ml.

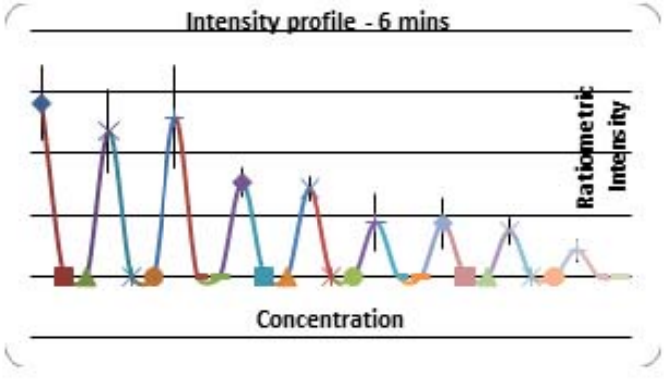

Figure 15. Relative color intensity of test line at 6 mins from blank to 1.0 mg/ml

- **Optimization of assay tim**e

Given that the color change of the test line is related to the flow rate of samples, a series of experiments at different time periods have been conducted to understand the time effects on the color intensity change and, hence, the optimized sensitivity of the lateral flow strips. For example, slow flow rate may allow the sufficient binding of analytes to antibody, therefore improving sensitivity; however, the longer time will decrease the response time of the sensors. We monitored the changes of color intensity on the testing line at different time periods ranging from 2 minutes to 30 minutes (Figure 16).

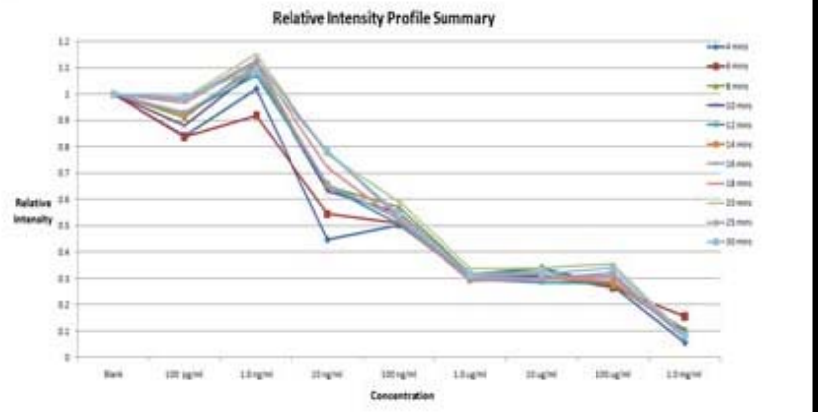

Figure 16. Relative color intensity of 8-OHdG standards at 11 time periods from blank to 1.0 mg/ml, indicating that 5-6 minute time periods are required to give an optimized the sensitivity.

Conclusion: Minimum 5-6 minutes time periods are required to give the optimized color change and, hence, optimized sensitivity of the detection system.

2.2.4. Electrochemical Detection Of 8-OHdG Using Screen-Printed Sensing Electrodes

For better quantitative information of the analyte (8-OHdG), we proposed integrating electrochemical sensing system to the lateral flow strips.

- **Fabrication of screen-printed electrodes:** Screen-printed electrodes have been fabricated using different electrode materials and different substrates (Figure 17).
- **Silver-based screen electrodes**: Silver ink has good conductivity but many researchers have shown silver to be toxic to biological samples.

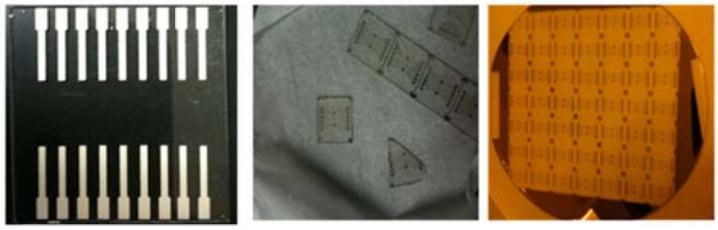

Figure 17: Different screen-print/thin film electrodes on various substrates.

- **Carbon ink screen-printed electrodes:** Carbon electrodes are as conductive as silver ink, but generally carbon is easily absorbed by biological molecules, thus weakening the electrochemical activity of the electrodes (Katz, 1994). However, the carbon ink we selected is not only conductive, but also solvent resistant, thus making it compatible for further surface modification, cleaning and reusability.
- **Gold thin-film electrodes:** Different from the screen-printed electrodes, gold thin-film electrodes on glass substrates have been fabricated using traditional photolithography**.** The microchip consists of Pyrex glass wafer as the platform, gold thin film electrodes as the sensing and signal transmitting mechanism, and SU-8 as the passivation layer.
- **Commercialized screen-printed electrodes:** Various **c**ommercialized electrodes (Figure 18) constructed by more advanced nanomaterials include graphene electrodes, Gold Nanoparticle decorated electrodes, carbon nanotube electrodes (CNTs). These have been used for optimization of 8-OHdG electrochemical detection. Performances, including sensitivity and reproducibility of commercialized electrodes on the 8-OHdG electrochemical measurements, have been compared to the home-made screen-printed electrodes. CNTs and graphene based electrodes in particular have been reported to be very electrochemically active for highly sensitive detection of biological species.

Figure 18: Commercialized screen-printed electrodes made by carbon, graphene, carbon nanotubes, and other materials.

- **Hydrodynamic Study Of 8-OHdG In PBS Buffer Solution**

To determine the effects of electrode materials on the electrochemical activities of 8-OHdG, electrochemical measurements of 8-OHdG in buffer solution were carried out using the previous described electrodes (Figure 19). Sensitivity, hydrodynamic ranges and response time of electrodes toward 8-OHdG detection were compared using cyclic voltammetry and chronoamperometry, two major electrochemical techniques for measurements. Gold Nanoparticle-modified carbon electrodes have so far shown an optimized current value of 8-OHdG compared to other types of electrodes. However, the long term stability of the electrodes is not sufficient, presumably due to oxidation of Gold Nanoparticles or physical absorption of the biomarker or other molecules.

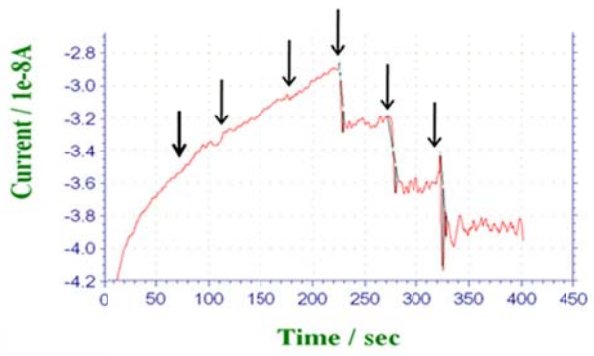

Figure 19. Arrows in the graphs show the application of (PBS/8-OHdG) solution in the container. The first arrow at 75 s shows the application of PBS buffer signal change observed. The second and third arrow (100 s and 175 s, respectively) with 10 ng/ml 8-OHdG solution shows a change in signal. The last 3 arrows (respectively 225 s, 275 s and 325 s) ng/ml of 8-OHdG solution, which results in a greater signal change.

- **Electrochemical Measurement Of 8-OHdG On Natural CellulosePaper**

Electrochemical response of 8-OHdG saturated cellulose paper was also tested using the screen-printed electrodes. Each paper was pre-treated by 8-OHdG solutions in variable concentrations and placed on the screen-printed electrode. Cyclic voltammetry was conducted to measure the electrochemical response of 8-OHdG biomarker. Figure 20 shows significant oxidization currents at 0.60 V vs. Ag/AgCl, gradually increasing with increasing 8-OHdG concentrations from 100 pg/ml to 10 µg/ml. Our data indicate that 8-OHdG also shows strong electrochemical activities on 8-OHdG absorbed on papers, providing the basis for detecting 8-OHdG using screen-printed electrode-integrated paper strips.

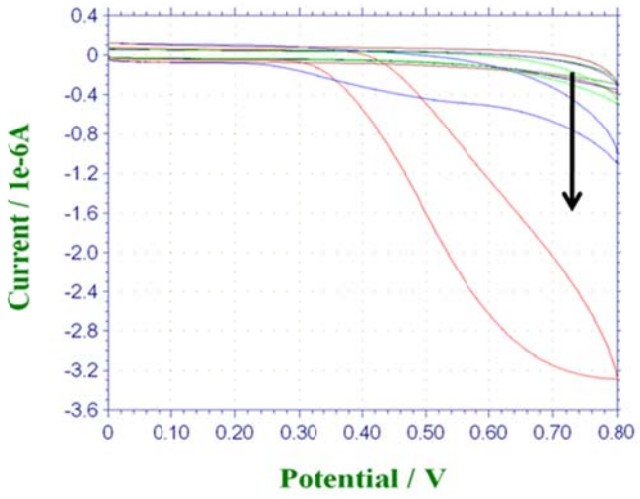

Figure 20. Cyclic voltammogram of 8-OHdG absorbed on natural cellulose papers. The arrow indicates the increase of oxidization current of 8-OHdG when gradually increase the 8-OHdG concentration ranging from 100pg/ml to 10 µg/ml

2.3. SERS Based Gold Nanoparticle Whole-Cell Biosensor

OVERALL OBJECTIVES: The overall goal of the project is to develop a whole cell SERS sensor for the toxic exposure assessment, based on metal nanoparticle that detect and quantify the expressed stress proteins Hsp70, Rad54 and Caspase-3 in yeast cells.

2.3.1. Measure Hsp70, Rad54 And Caspase-3 Expression In Yeast Cells Exposed To Various Toxicant/Stress Using Existing Conventional Technique Enzyme-Linked Immunosorbent Assay (ELISA)

Two crude fresh yeast samples were purchased from Kosher Kingdom bakery and Red Star Company. Because of comparative high purity (evident from smell, chemical composition and Agar plating), Red star yeast cultures were chosen for the research work. The crude culture was characterized morphologically on the basis of shape and color of microbial colonies to obtain highly pure yeast cells using serial dilution, Agar plating and streaking methods removing mold and reducing bacterial contamination. Stored and characterized yeast cultures were revived and grown in dehydrated YPD Broth media for 72 hrs. at 30°C. Indirect (Spectrophotometric absorption at 600nm) and Direct (Colony count) methods were used to determine concentration of budding yeast. Cell-lysate was prepared using combination of chemical extraction and freeze thaw methods and protease inhibitor cocktail to obtain ultrapure total protein from cultured yeast cells. Purity of total protein extracted was analyzed

spectrophotometricaly, taking characteristic maximum absorption at 280nm, before quantitating total proteins and specific stress proteins using commercial ELISA kits.

- **Characterization of crude yeast**

Crude yeast grown on YPD Agar media resulted in a mixture of microbial colonies. Filamentous fuzzy molds were easily distinguished from yeast and bacterial colonies, which were almost always similar and could be distinguished on basis of their color and thickness. Yeast colonies are white and more solid, compared to bacteria which are yellow and less dense. Identified yeast colonies were picked up, streaked on agar plates to increase their number and pour-plated to yield pure white solid yeast colonies (Figure 21).

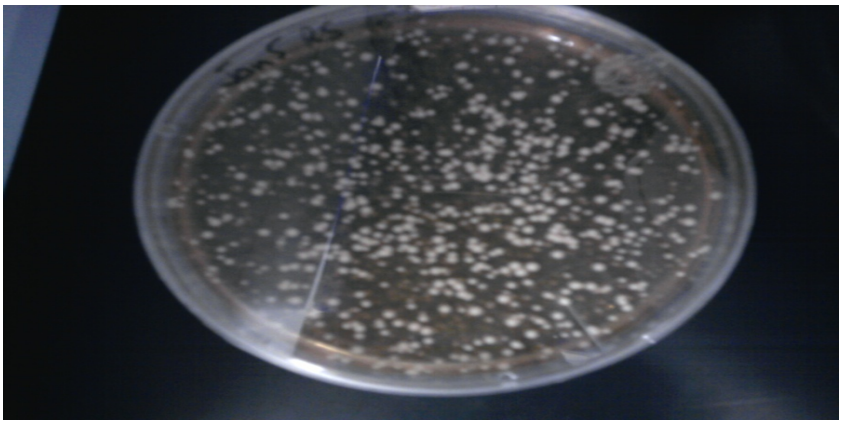

Figure 21. Photograph of pure yeast colonies (Morphological Characterization) void of contaminants

- **Estimation of Yeast concentration**

Yeast concentration is estimated by two methods

(i) Indirect spectrophotometer method measuring absorption at 600 nm and using Beer Lambert's law: $A = \varepsilon \iota c = 1x10^7$ cells/ml

(ii) Direct method (colony count)

$$\frac{No\ of\ colonies\ x\ Dilution\ factor}{Volume\ of\ Aliquot\ (ml)} = \frac{30x10^3}{0.1} = 3\ x\ 10^5\ CFU/ml$$

- **Purity analysis of extracted total proteins**

Purity of protein extracted from yeast was assessed spectrophotometrically (Figure 22). Maximum absorption at around 280 nm and an absorbance ratio A280/A260 of 1.5 indicates that cell-lysates have ultra-pure proteins free of DNA contamination. Total proteins extracted from yeast cells were quantified using Bovine Serum Albumin (BSA) as standard (Figure 23). A total of 10^7 yeast cells/ml yield 60µg of total proteins (60µg/ml).

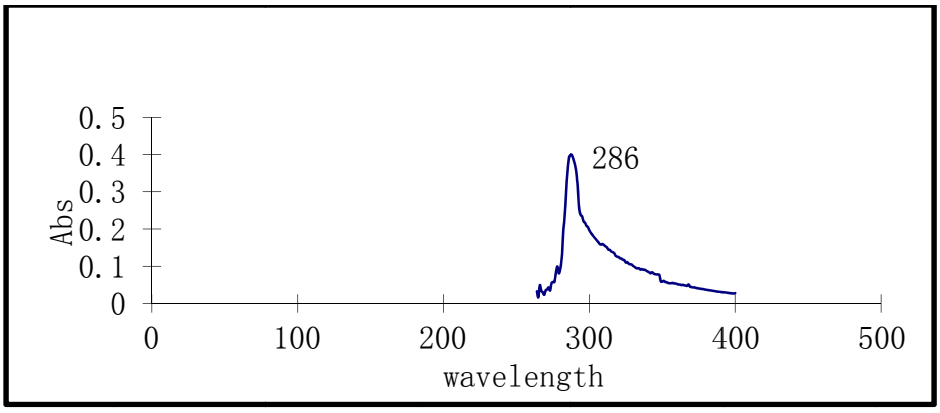

Figure 22. Absorption Spectra of Yeast Cell-lysates for protein purity analysis (Absorption @ 280/ absorption @ 260 nm = 0.8534/0.5503 = 1.5)

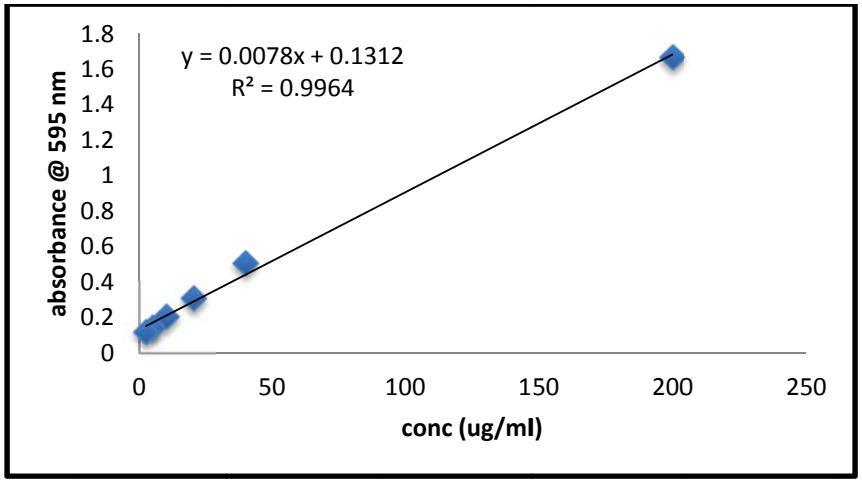

Figure 23. Bovine serum albumin standard Curve

- **Quantitation of stress proteins expressed in yeast cells after exposure to toxins (dose and time kinetics)**

The same batch (10^7 cell/ml), quantified for total proteins, was subjected for analysis of specific stress proteins: Hsp70 Rad54, and Caspase. Dose and time-dependent studies were done in order to correlate them with toxicant exposure level and duration. Three (3) doses and 2 times were chosen to study the effect of two common environmental toxins/stress: H_2O_2 (5mM, 50mM, 500mM doses for 20 and 60 mins each) and UV (A 365 nm, B 302 nm, C 254 nm doses for 5 and 15 mins each). Experiments were repeated three times, loading samples in duplicate each time (n= 3x2) and graphically represented in terms of mean ± standard deviation. Caspase-3 was not detectable. Results for Rad54 (Figures 24A&B) and Hsp70 (Figure 25A&B) are shown.

I) Response of Rad54 stress protein to toxins (dose and time kinetics)

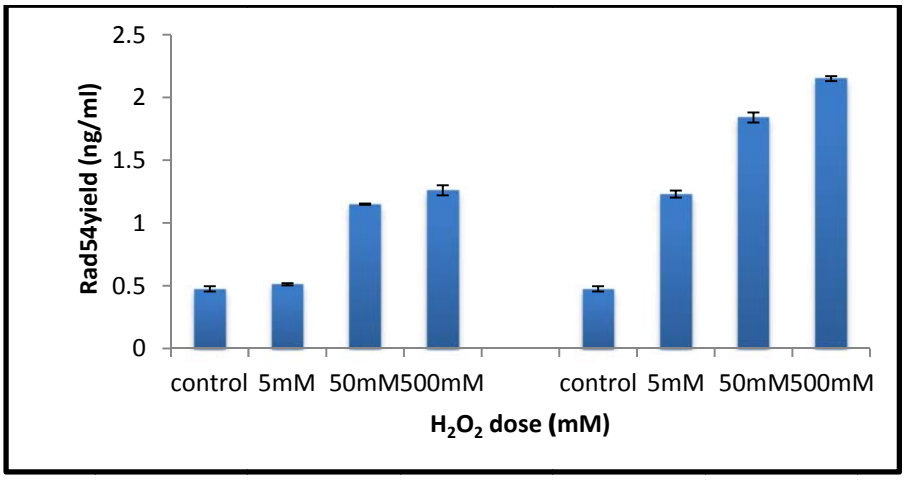

Figure 24A. ELISA quantitation of Rad54 expressed in yeast cells exposed to the toxin H_2O_2. Left Panel: 20 minutes exposure time Right Panel: 60 minutes exposure time. Control: cells under no stress/toxin (non-induced cells)

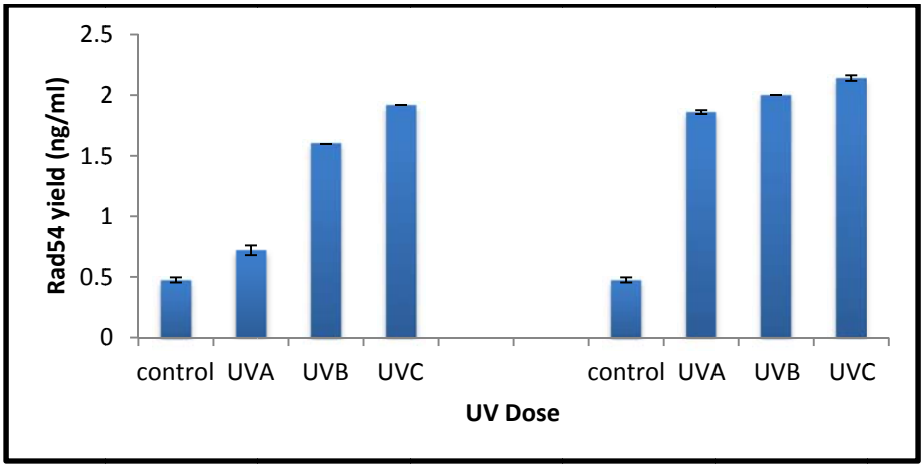

Figure 24B. ELISA quantitation of Rad54 expressed in yeast cells exposed to the toxin UV. Left panel: 5 minutes exposure time Right panel: 15 minutes exposure time. Control: cells under no stress/toxin (non-induced cells)

We conclude that non-induced control cells under no stress and having base expression of approximately 400 pg/ml show, when exposed to toxins hydrogen peroxide (Figure 24A) and UV (Figure 24B), increased expression of Rad54. Expression increases with increasing dose and time until reaching saturation (expression potential) at 2.15 ng/ml Rad54 stress proteins.

II) Response of Hsp70 stress protein to toxin

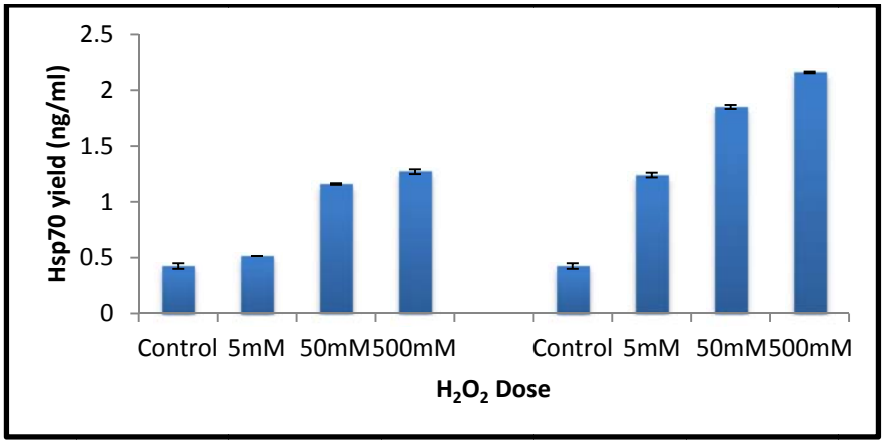

Figure 25A. ELISA quantitation of Hsp70 expressed in yeast cells exposed to the toxin H_2O_2. Left Panel: 20 minutes exposure time Right Panel: 60 minutes exposure time. Control: cells under no stress/toxin (non-induced cells)

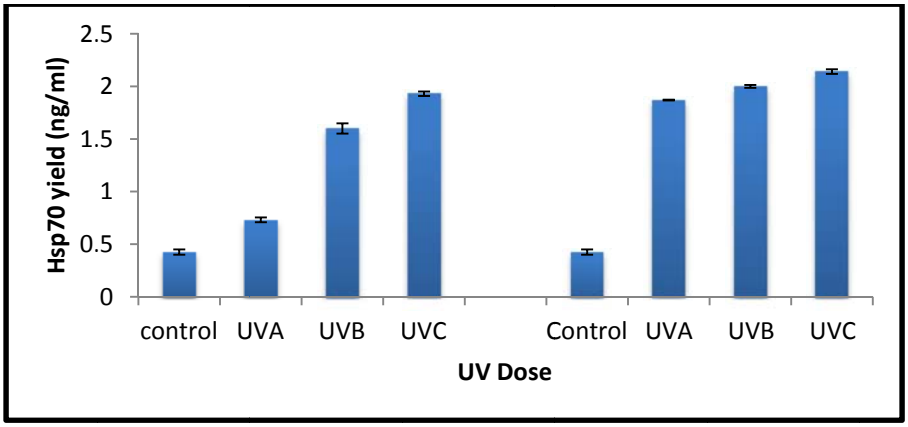

Figure 25B. ELISA quantitation of Hsp70 expressed in yeast cells exposed to the toxin UV. Left panel: 5 minutes exposure time Right panel: 15 minutes exposure time. Control: cells under no stress/toxin (non-induced cells)

We conclude that non-induced control cells under no stress and having base expression of approximately 300 pg/ml when exposed to toxins hydrogen peroxide (Figure 25A) and UV (Figure 25B) show increased expression of Hsp70. Expression increases with increasing dose and time until reaching saturation (expression potential) at 2ng/ml Hsp70 stress proteins.

- **Caspase detection in yeast**

The same batch of samples/lysates with 10^6 cells/ml were studied for Caspase-3 expression using the Sigma commercial ELISA kit compatible with human cells. No Caspase-3 expression was detected in yeast cells. To confirm experiment validity, the standard Caspase-3 antigen was loaded in every experiment. Yeast-compatible trial kits from ICT were purchased to detect Caspase-3 and/or polyCaspase (whole Caspase family). Again, no Caspase was detected, indicating that either the Caspase expression in yeast cells is very low (below the lower sensitivity of the commercial kit) or incompatibility exists between the kit and this particular strain of yeast (*Saccharomyces cerevisiae*). These two ideas

were supported by the literature. Caspase ortholog metaCaspase Yca1p is the primary Caspase-like protein responsible for apoptosis in yeast cells, but all Caspase-like proteases in total contribute only 40% to yeast cell death; the remaining 60% involve are by Caspase-independent pathways. We conclude the Caspase protein is present only in very little amounts in yeast, and thus not an attractive analyte for our work.

2.3.2. Optimize The Fabrication Of The Gold Nanoparticle Sensor For Detection Of Hsp70, Rad54 and Caspase-3 Using SERS

- **Gold nanoparticle as SERS substrate (Gold NP – 1)**

Octahedra Gold Nanoparticles were synthesized according to an established synthetic procedure (Kim et al., 2009) and characterized for their size, shape and optical property. Figures 26, 27 and 28 show the LSPR spectrum, transmission electron microscopy (TEM) image, and DLS histogram of the synthesized octahedra Gold Nanoparticles. Sizes of the nanoparticles obtained are estimated to be 80±8nm.

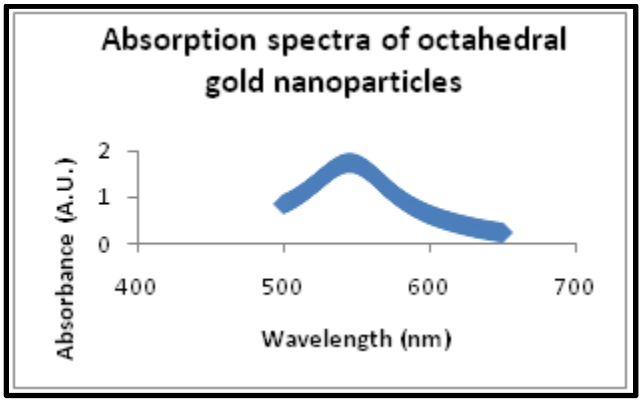

Figure 26. UV-visible spectrum of octahedra Gold Nanoparticle

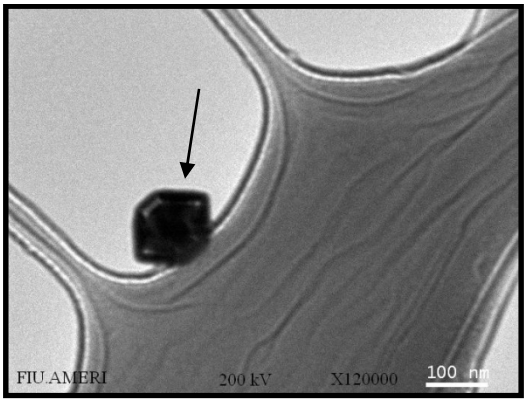

Figure 27. TEM image of octahedra Gold Nanoparticle (arrow). The particle appears to be six-sided in this figure (2D) but has additional sides in 3D.

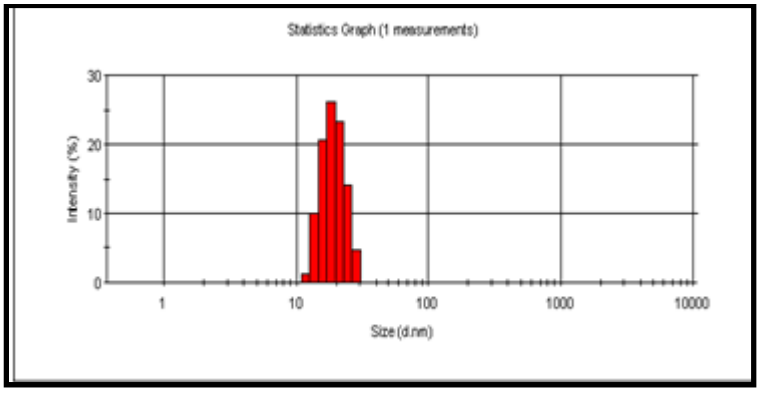

Figure 28. Size distribution of octrahedra Gold Nanoparticles by Dynamic Light Scattering method

- **SERS of 0.5µM of Rhodamine B**

Synthesized Gold Nanoparticles were tested for SERS activity using the standard Raman dye Rhodamine-B at a concentration of 0.5µM. Figure 29 shows the corresponding SERS spectrum of Rhodamine B. The SERS enhancement factor was estimated to be in the order of 10^4.

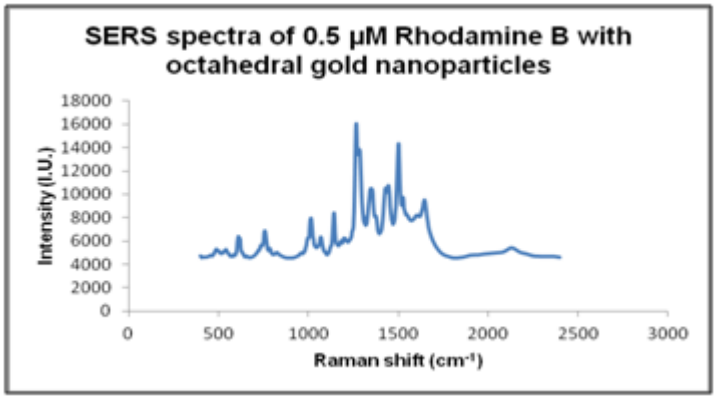

Figure 29. SERS spectrum of Rhodamine B (0.5µM)

- **SERS of Hsp70 protein using Gold Nanoparticle conjugate**

The linker molecule MMT was chosen as the cross-linker to bind antibody to the Gold Nanoparticle. Antibodies against the stress protein Hsp70 and Caspase-3 were successfully attached to the Gold Nanoparticle via linker molecule and further interacted with Hsp70 and Caspase-3 proteins. In order to determine the optimal concentration of antibody for coating the surface of the nanoparticle, a conjugation efficiency study was conducted. Nanoparticles were coated with optimal number of antibodies, therefore in turn the binding protein experiencing maximal electromagnetic enhancement from the nanoparticle. The optimal molar ratio of the proteins, Hsp70 and Caspase-3 was found to be 100 and 70 respectively. The number of antibodies per nanoparticle was estimated to be 201/nanoparticle. Figure 30 shows the SERS spectrum of the stress protein Hsp70 bound to the Gold Nanoparticle conjugate. Although the particles show quite appreciable amount of enhancement, this failed to produce Raman signal of the protein of interest was not observed. Additional work is necessary to identify appropriate linkers and nanoparticles material, size and shape to allow sensitive and specific measurement of the proteins using the SERS method and gold. In addition to gold, we are also investigating silver as a potential SERS substrate material.

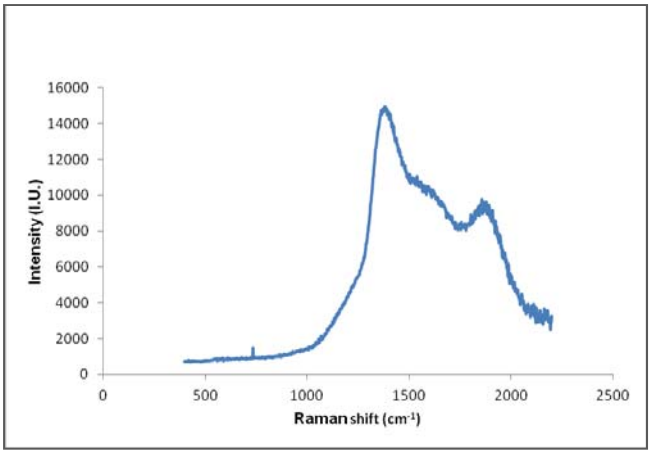

Figure 30. SERS spectrum of Hsp70-anti Hsp70-Gold Nanoparticle complex

- **Silver nanoparticle as SERS substrate**

To date there is no published literature reporting the detection of the stress proteins Caspase-3, Rad54 and Hsp70 using SERS. We were able to detect successfully all three stress proteins in their standard form using colloidal silver nanoparticles as SERS substrates. Gold Nanoparticles are biocompatible and known for the ease of functionalization with other biological molecules. In addition, gold possesses surface plasmon oscillating ability with the frequency in the (Near Infrared) NIR region and, hence, excitation with NIR laser radiation is possible. Although Gold Nanoparticles are expected to produce an appreciable amount of signal when excited with NIR laser source, we have found it challenging to obtain the SERS signal of interest so far. To determine if the stress proteins produce identifiable and specific Raman signal, we attempted to determine the SERS potential and characteristic Raman bands for Hsp70, Rad54 and Caspase-3 stress proteins. Silver nanoparticles were thus utilized. In general silver nanoparticles in comparison to gold produce high resolution and high intensity SERS signal due to their size, shape, roughness and dielectric property. All favorably exert a SERS effect. A 3-D colloidal silver nanosphere-based SERS substrate was thus synthesized and investigated. Although silver is known to have antibacterial properties, it is possible that yeast cells may be more resistant to the effects of silver. A compatibility study on yeast cell up-take of silver nanoparticles will be required, and initiated. Nevertheless, our preliminary goal in using silver nanoparticles is to identify whether SERS of the stress proteins could be accomplished and to identify their characteristic Raman band.

In these set of experiments we utilized the method of label-free detection of stress proteins of known concentrations so that the optical response (SERS signal) would be in proportion to the number of antigens (stress proteins). We expect that nanoparticles tagged with antibodies specific to target proteins (antigen) will produce a higher SERS signal than the method without specificity in detection, given greater number of interactions between the antigen and the nanoparticles. Therefore, in the next phase nanoparticles will be tagged with specific antibodies. In this report label free detection method without specificity in detection is presented.

- **Synthesis of 3-D Silver colloidal nanosphere**

The synthesis (Bai et al., 2007) of nanospheres is a bottom-up assembly technique in which nanospheres are produced in two stages. In the first step, tiny nanocrystals were synthesized, and in the second step the produced nanocrystals were assembled into less dispersible colloidal nanospheres by the use of surfactant and low boiling solvent. Synthesis of nanocrystals is a liquid-solid-solution phase transfer synthetic process, whereby in general Ag^+ ions are reduced at the interface of solid-liquid and solid-solution phases during the reaction mixture. Due to the hydrophobic (linoleic acid) and hydrophilic surrounding (ethanol, water), and because of the gravitational pull, reduced Ag^+ ions (Ag) settle to the bottom of the vial at the latter stage of the 24hour synthesis process. Resulting silver nanocrystal precipitates were collected, centrifuged with ethanol, and dispersed in cyclohexane solvent in preparation for the synthesis of colloidal spheres.

The product (3-D Silver colloidal nanospheres) is obtained by the oil in water (O/W) micro-emulsion based approach. The microemulsion oil droplet (oil phase) is formed when the linoleic acid protected nanocrystals is dispersed in water. The oil droplet contains the tiny nanocrystals and low boiling point solvent (cyclohexane), whereas the aqueous phase contains water and the surfactant (sodium dodecyl sulphate) that stabilizes the nanocrystals by hydrophobic interaction. On heating the reaction mixture, cyclohexane in the oil phase evaporates, causing the oil droplet to condense and have the nanocrystals stick to each other forming colloidal nanospheres.

- **Characterization of Silver colloidal nanosphere**

The synthesized silver colloidal spheres were characterized for this morphological and localized surface plasmon resonance (LSPR) properties. The TEM image in Figure 31 shows the shape and size distribution of the colloidal silver nanosphere particles. The particle size is estimated to be 34±7nm and the particles are spherical in shape. The low standard deviation (error) indicates that the particles have a small size distribution and therefore could possess better SERS activity.

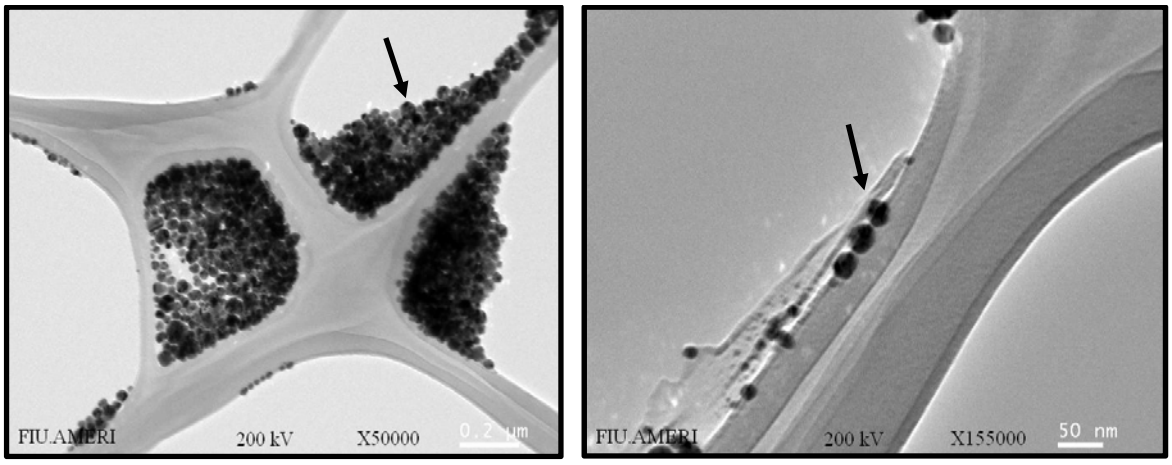

Figure 31. TEM images of 3-D Silver colloidal nanosphere (arrows)

To confirm the formation of silver colloidal spheres, the corresponding LSPR spectrum was obtained. The extinction spectrum in Figure 32 confirms that colloidal nanospheres were formed. Silver

nanocrystals exhibited a sharp plasmonic peak at a lower wavelength of 391nm compared to silver colloidal spheres with a broad peak red shifted to 441nm. Also, comparison of the two absorbance profiles indicates that the colloidal spheres were larger in size (broad peak and at higher wavelength) compared to silver nanocrystals (sharp peak and at lower wavelength). This explains the corresponding redshift.

Figures 33 show the SERS spectrum of Caspase-3 at a concentration of 250ng/ml. Figure 34 shows the SERS intensity profile at a concentration range 0 to 250ng/ml of standard Caspase-3 proteins. Intensity (Raman band centered at 725cm^{-1}, corresponds to the Amide IV functional group of Aspartic acid), for each concentration increases in proportion to the concentration of Caspase-3. Results indicate that the silver colloidal nanospheres may be a good substrate for the detection of Caspase-3 for the case of protein quantification within the yeast cells. Figure 35 shows the dose response behavior for the silver colloidal nanospheres in detection of Caspase-3 proteins. We are able to successfully detect Caspase-3 at a concentration of 0.2ng/ml where the typical yield of Caspase-3 in the yeast cells is believed to be in the range of 0.4ng/ml-2.5ng/ml. **We are able to detect 1ng/ml of Caspase-3 using SERS at levels below the level of detection of the commercial ELISA kit (4.8ng/ml).**

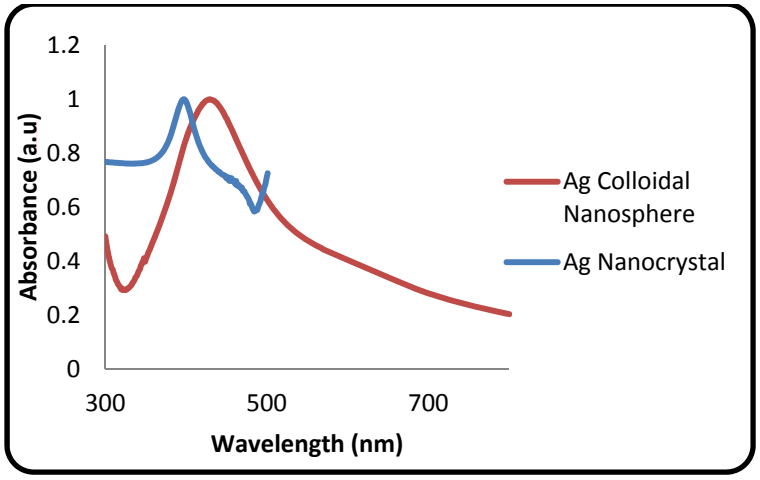

Figure 32. UV-visible absorbance spectrum of 3-D Silver colloidal nanosphere

- **Quantification of standard form of stress proteins**

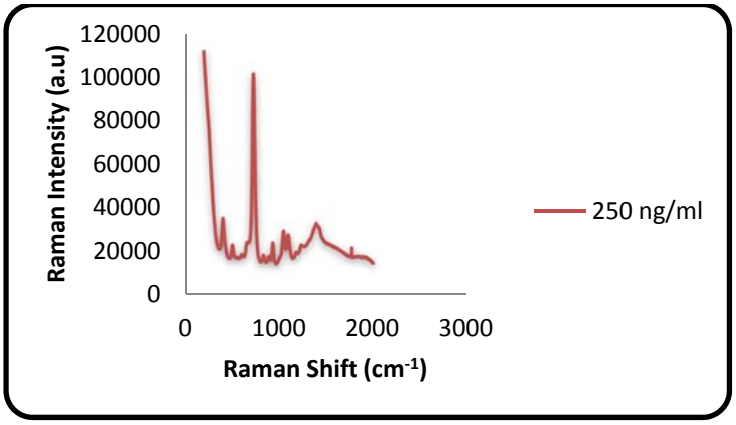

Figure 33. SERS spectrum of Caspase-3 at a concentration of 250ng/ml

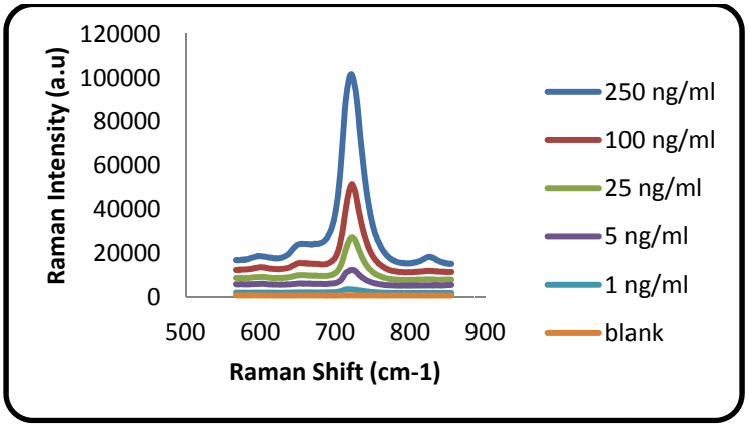

Figure 34. SERS intensity profile at various concentrations of Caspase-3

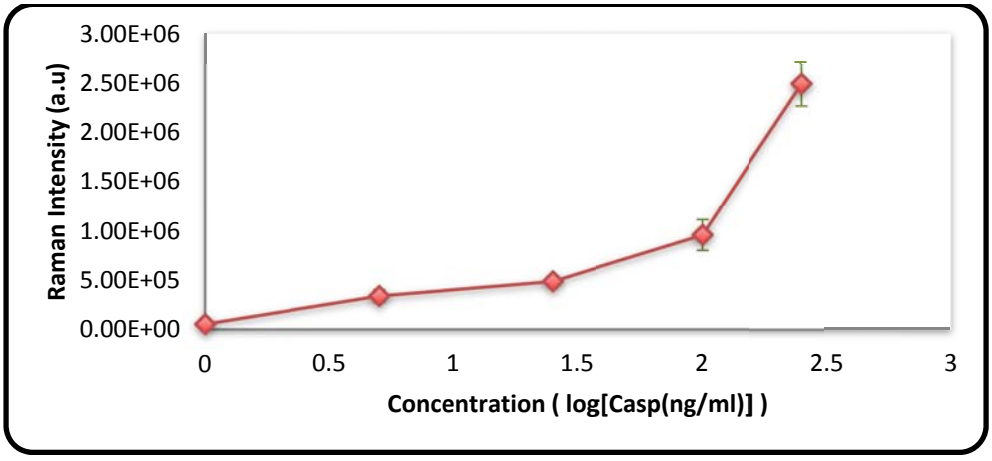

Figure 35. Dose response curve at various concentrations (ng/ml) of Caspase-3

Figure 36 shows the dose response behavior for the silver colloidal nanospheres in detecting Rad54 proteins. Intensity is calculated from the Raman band centered at 1394cm^{-1} in the corresponding SERS spectrum.

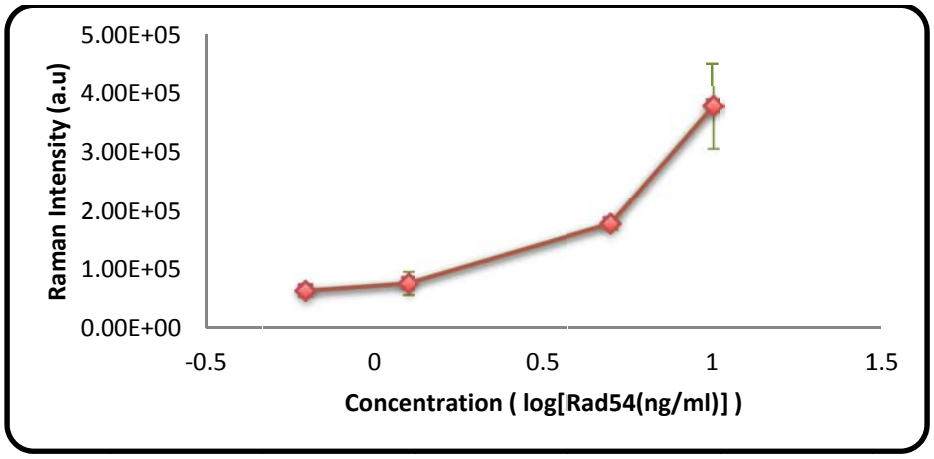

Figure 36. Dose response curve at various concentrations (ng/ml) of Rad54

Figure 37 shows the dose response behavior for the silver colloidal nanospheres in detecting Hsp70 proteins. Intensity is calculated from the Raman band centered at 757cm^{-1} in the corresponding SERS spectrum. Saturation of Raman signal is observed when the concentration of Hsp70 is above 3.25ng/ml.

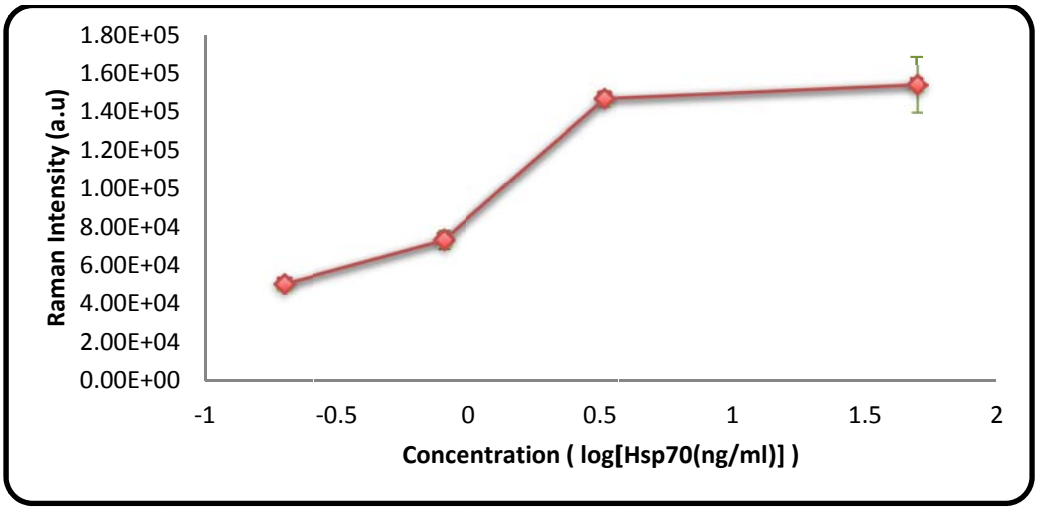

Figure 37. Dose response curve at various concentrations (ng/ml) of Hsp70

- **Silver as an alternative to gold colloid nanoparticles as SERS substrate**

Because we were able to detect successfully the stress proteins using silver colloidal nanospheres, it is evident that Raman signal might be emitted from Gold Nanoparticles. In this respect two different alternate Gold Nanoparticles were synthesized in parallel, after an initial effort using gold colloids proved unsuccessful in detecting the analytes. These methods are likely to result in nanoparticles with rougher surfaces and sharp edges which are more likely to enhance Raman scatter compared to particles with smooth surface (i.e., colloids).

- **Gold NP – 2: Seed mediated growth of high purity octahedra Gold Nanoparticle**

A facile method (Kim et al., 2011) for the synthesis of gold octahedra nanoparticles was selected to produce particles of well controlled size, shape and optical property. The synthesis is a three step process, with the first two steps focused on the synthesis of single-crystal spherical gold seeds and the final step the synthesis of gold octahedra nanoparticles. Starting with a single-crystal seeds of gold spheres, uniform gold octahedra particles can be obtained with a narrow size distribution (<7%) and in high purity (>90%). Size of the octahedra nanoparticles could be tuned from 16 to 77nm by varying the amount of seed and concentration of gold precursor salt.

We were able to accomplish the synthesis of gold spherical seeds by successfully carrying out the initial two steps. Figure 38 shows the red color seed solution obtained as the result of the synthesis. The LSPR spectrum obtained in Figure 39 matches with data in the literature, further confirming that the seed solution has been produced successfully. However, we are not yet successful in the final step in the synthesis of gold octahedra nanoparticles as no color change or precipitation were observed, the sine qua non for confirming colloidal gold octahedra nanoparticle solution. This indicates the need for further optimization of synthesis parameters, such as stirring, access to air, temperature and the concentration of $HAuCl_4$, PVP and spherical gold seeds. Directions towards the optimization of the above mentioned parameters are being pursued.

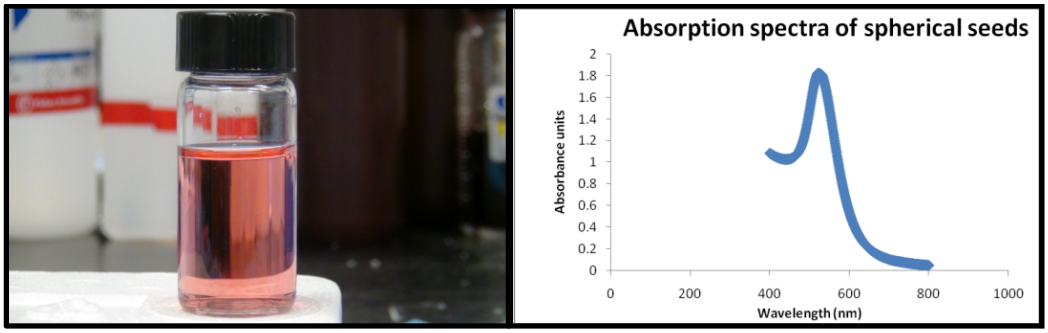

Figures 38 and 39. (Left) Gold spherical single-crystal seed solution showing appropriate color and density indicating successful production of the gold spherical seeds. (Right) UV-visible absorbance spectrum of gold spherical seeds.

- **Gold NP – 3: Gold colloidal nanospheres**

Gold colloidal nanospheres were synthesized similarly to that for silver colloidal nanospheres but with variations. The hot injection-based method (Wang et al., 2008; 2011) was utilized for the introduction of gold precursor salt into the octadecylamine (ODA) system, with the period of synthesis kept very short. At elevated temperature (160^{o}C), ODA offers free electrons to Au^{3+} ions, aiding in the reduction of gold metal ions. The synthesis involves two steps, 1) gold nanocrystals synthesized, and 2) colloidal sphere generation by assembling of gold nanocrystals using surfactant (SDS, CTAB) and low boiling point solvent (cyclohexane).

Figure 40 shows the LSPR spectrum of the obtained Gold colloidal nanospheres. The absorbance maximum is found to be approximately 530nm, the characteristic absorbance maximum for Gold

Nanoparticles. As seen in Figure 41 the color of the synthesized gold colloidal sphere turned reddish, further confirming the formation of gold colloidal spheres. Particles were quickly tested for SERS activity with standard and routine chemicals, such as Rhodamine 6G, 4-Aminothiophenol and Rhodamine B. None were successful. The reason could be dilution, collected gold precipitates (gold nanocrystals) were diluted in 100ml water following centrifugation with the surfactant (SDS) and cyclohexane solvent for the nanosphere formation. We were, however, able to obtain a thick precipitate of gold particles of higher yield. Addition of surfactant to CTAB to increase yield will be tried.

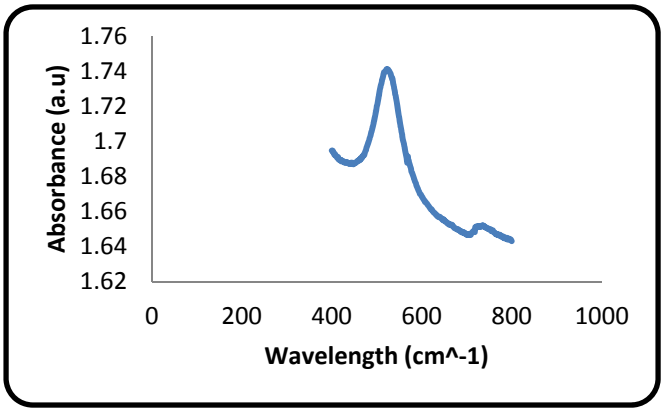

Figure 40. UV-visible absorbance spectrum of gold colloidal nanospheres

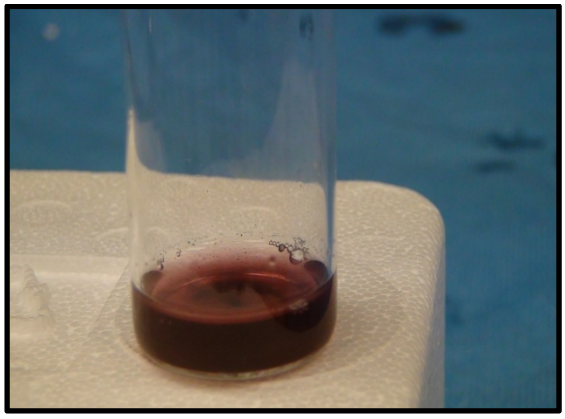

Figure 41. Gold colloidal nanosphere solution

- **Problems Encountered**
  - **Problem 01 -** SERS of stress proteins both in free form and bound to the antibody-gold nanoparticle complex has not yet been accomplished using octahedra (Kim et al., 2009) shaped Gold Nanoparticle (Gold NP – 1)
  - **Problem 02 -** Although red-colored single crystal Gold spherical seed solution was prepared, no characteristic color change or precipitation of particles occurred in the final phase of the octahedra Gold Nanoparticle (Kim et al., 2011**)** synthesis (Gold NP – 2)
  - **Problem 03 -** Prepared gold colloidal nanospheres using the technique described by Wang et al., (2008; 2011) were not SERS active (Gold NP – 3)
- **Proposed Solution to Problems Encountered**
  - **Solution 01 –** Lack of required SERS enhancement from the gold as compared to silver nanoparticle. Alternative Gold Nanoparticle synthesis methods will be sought that yield less dispersed, but denser colloidal suspension. Monodisperse and dense colloidal nanoparticles could possibly create nanoparticle clusters and reproducibly maximize SERS enhancement.
  - **Solution 02 –** Optimization of the synthesis procedure through experiments modifying molar ratio of PVP (poly-vinylpyrrolidone) to $HAuCl_4$, deviating from the original value (661:1) under controlled temperature and optimal stirring velocity.
  - **Solution 03 –** Although (visually) dense gold colloidal suspensions were obtained, dilution of the concentrated particles obtained after centrifugation −with 100ml of DI water may have caused the particles to become too dispersed. To avoid this, the collected particle after

centrifugation will be diluted or dispersed in only 5-20 ml DI water and then evaluated for SERS activity.

- **Alternate methods to reach goals**

Due to the difficulty in the detection of stress proteins of interest (Hsp70, Caspase-3 and Rad54) using Gold Nanoparticles, it was critical and necessary to achieve Raman activeness of the stress proteins, requiring sufficient electromagnetic and or chemical enhancement. Consequently 3-D silver colloidal nanosphere particles were synthesized and evaluated for the SERS potential of the stress proteins. Because silver particles are highly active, and realizing the stress proteins are Raman active, we became interested in extending the study to evaluate the bio-compatibility of silver nanoparticles within the yeast cells. We presume that because the yeast cells can survive hard and extreme environments, the chances of cells being bio-compatible are good.

3. Key Research Accomplishments

3.1. Cytogenetics Assays

- Completed IRB documentation to enable collection of human blood samples and subsequent approval
- Recruited successfully nine subjects to participate in the study
- Established the parameters for culturing human lymphocytes
- Finalized the process for defining dose response of lymphocytes to H_2O_2
- Initiated and established protocols for the CA assay
- Identified chromosome aberrations at all exposure concentrations of H_2O_2 (25-200µmol/ml). Clear associations have been found with increasing numbers of aberrations and severity of aberrations with increasing H_2O_2 concentrations
- Established FISH protocols for various commercially available FISH probes in lymphocyte nuclei and chromosomes suitable for use in combination with the DNA damage assays

3.2. EIST Based Biomarker Sensor For Oxidative DNA Damage Assessment

- Initiated and established protocols for conjugating and characterizing antibody and Gold Nanoparticles
- Established protocols for the fabrication of lateral flow strips for the detection of bacterial cells and 8-OHdG biomarker
- Developed a sandwich-type immuno lateral flow strip for multiplex bacterial cells detection
- Demonstrated that 8-OHdG molecules have single antigenic sites, suitable only for competitive type-based immuno lateral flow strip detection
- Tested the feasibility of detecting 8-OHdG using lateral flow immuno strips based on the competitive immuno assay
- Detected 8-OHdG semi-quantitatively in buffer solution in ranges 1 ng/ml to 1 mg/ml

- Fabricated different mateirals based screen-printed electrodes using nano/micro fabrication techniques
- Meatured electrochemcial activites of 8-OHdG using the fabricated electrodes
- Compared the electrochemical reponse of 8-OHdG on different electrode surfaces and found that the Gold Nanopartcles decorated carbon electrode provided optimized electrochemcial signals
- Demonstrated the electrochemcial activies of 8-OHdG on wet papers

3.3. SERS Based Gold Nanoparticle Whole-Cell Biosensor

- Completed dose and time kinetics study to quantify the expressed stress proteins - Hsp70 and Rad54, in response to environmental stress H_2O_2 and UV using ELISA
- Measured standard forms of Caspase-3, Rad54 and Hsp70 proteins using 3-D silver colloidal nanosphere as SERS substrate
- Measured 1 ng/ml of standard forms of Caspase-3 proteins using SERS below the level of detection of commercial ELISA kits (4.8ng/ml)

4. Reportable Outcomes

4.1. Cytogenetics

Dr. Tempest was awarded a funded place and participated in the short course on Genomics held at the National Institutes of Health National Human Genome Research Institute (NHGRI). Bethesda July 24th-29th 2011.

Dr. Simpson and Dr. Martin were invited speakers at International Chromosome Conference and have been speakers in other venues nationally and internationally.

4.2. EIST Based Biomarker Sensor For Oxidative DNA Damage Assessment

Journal Publications

Li, C-Z., Vandernberg, K., Prabhulkar, S., Zhu, X., Schneper, L., Mathee, K., Rosser, C.J., Almeide, E., Paper based point-of-care testing disc for multiplex whole cell bacteria analysis, Biosensors and Bioelectronics, 26, 4342-4348, 2011.

Conference Presentations

C.-Z. Li, "Biosensing Strip for Whole Cell Pathogenic Bacteria Detection", November 15th-19th, 2010 Chemical & Biological Defense Science and Technology Conference (CBD S&T Conference), Orlando, FL.

X.Zhu, C.-Z. Li, "Paper based point of care testing sensor for DNA oxidative damage biomarker detection", Sep 30-Oct 1st, NanoFlorida 2011, Miami, Florida,

4.3. SERS Based Gold Nanoparticle Whole-Cell Biosensor

Oral presentation in the ", Sep 30-Oct 1st, NanoFlorida 2011, Miami, Florida) "Sensitive and Label-Free Raman Detection and the Yeast Cellular Uptake of Colloidal Silver Nanospheres for In-vivo SERS Quantification of Caspase-3 Proteins". Authors: Joshy F. John, Vinay Bhardwaj, Supriya Srinivasan and Anthony J. McGoron

5. Conclusions

5.1. Cytogenetic Assays

We have been successful in achieving all first year project milestones outlined in the proposal despite delay in initiating experiments while awaiting IRB approval. Specifically, we have almost completed dose response experiments for exposure to H_2O_2. Using the CA assay we have demonstrated that all concentrations tested can elicit DNA damage. As anticipated we observed a reduction not only in mitotic cell index (cell proliferation), but also frequency and severity of DNA damage to be correlated with increasing concentration of H_2O_2. We are in the process of investigating the effect of additional H_2O_2 concentrations, specifically with the lower concentration 12.5µmol/ml, intermediate concentration 50µmol/ml, and a higher concentration 400µmol/ml. Following these experiments we will decide which of these will be included for future assays (CA, MN and comet). We are currently embarking on our initial experiments to determine the exposure ranges of the second genotoxic agent (UV) and anticipate that this should be completed relatively quickly. The project milestones include the MN assay as the first to be embarked upon. Given that the CA assay is the most laborious to analyze we have, however, embarked on this assay initially; while currently performing our initial validation experiments for the MN assay. Once the MN assay is established, we will initiate the Comet Assay validation experiments. Our FISH experiments have been successful with various FISH probes and can now be combined with the various DNA damage assays when they are validated. We will continue to validate different FISH probes throughout the project, all of which may be more specific to individual DNA damage assays. This will ultimately allow us to address fundamental questions regarding the type of DNA damage caused by specific genotoxic agents vis a vis sensitivity and specificity of two nanoscale biosensors being developed.

5.1.1. Future Plan

- Continue CA assay analysis of H_2O_2 treated lymphocytes
- Establish dose-responses for UV
- Validate and perform MN assay
- Validate and perform Comet assay
- Combine FISH with CA, MN assay and Comet assay
- Extend assay validation by use of other toxicants designated by DOD

5.2. EIST Based Biomarker Sensor For Oxidative DNA Damage Assessment

We demonstrated the feasibility of detecting 8-OHdG using lateral flow immuno strips based on the competitive immuno assay. Prior to our work, the DNA oxidative damage was primarily measured by traditional lab- based techniques such as HPLC and COMET. We can now use a disposable paper-based strip to assess the DNA damage by measuring the 8-OHdG biomarker.

We demonstrated feasibility of detecting 8-OHdG on papers using screen-printed electrodes, which provides the fundamental underpinning for integration of electrodes to paper strips for quantitative measurements of 8-OHdG. This pivotal step, is necessary for constructing of a biosensor to measure toxicant damage of unknown origin through ROS detection.

In summary, a sensitive and semi-quantitative method was established via use of gold particle-integrated competitive type lateral flow strips. Unlike a bacterial cell, which contains multiple antigenic sites, we demonstrated that the 8-OHdG is a single antigenic site molecule, and thus more suitable for competitive type lateral strips than sandwich type lateral flow strips. More quantitative analysis using different materials based screen-printed electrodes was then attempted. The best redox properties of 8-OHdG were observed using Gold Nanoparticle decorated carbon electrodes, although the long term stability of the electrode is still not sufficient. The current investigations thereby pave the way for a novel strategy for developing a sensitive paper-based analytical tool for oxidative DNA damage assessment. Moreover, the electrochemical study of 8-OHdG provides the fundamental basis for the future research plan of developing a more quantitative analytical method by integration of screen-printed electrodes to the paper-based lateral flow strips.

5.2.1. Future Plan

- Establish a protocol for biological sample collection, measurements and data analysis
- Validate the immune lateral strip for 8-OHdG detection using urine samples
- Improve the strip fabrication protocol using automation to improve the accuracy and reproducibility of the sensing system
- Develop a more efficient protocol to quantify the color intensity of the lateral flow system using image processing programs
- Improve the stability of screen-printed electrodes
- Integrate screen-printed electrode to the lateral flow strips
- Develop an integrated sensing system for electrochemical and optical detection of 8-OHdG
- Establish the correlation of experimental data based on both optical and electrochemical measurements in order to derive a realizable calibration curve for 8-OHdG detection.
- Validate of the sensing system by comparing our testing results to those of laboratory standard methods, namely COMET or HPLC-MS.

5.3. SERS Based Gold Nanoparticle Whole-Cell Biosensor

Working towards the goal of quantification of response of stress proteins in response to toxic exposures of yeast cells using SERS technique, gold and silver metal colloidal nanoparticles as SERS substrate were attempted. In this approach, octahedra gold nanoparticles (Gold NP – 1) have yet been convincing enough to be a superior SERS substrate. Thus, we sought alternate gold metal nanoparticle synthesis procedures. High purity and size controlled gold nano-octahedra (Gold NP – 2) and colloidal gold nanospheres (Gold NP – 2) synthesis procedures were obtained and subjected to optimization of synthesis parameters. It was crucial and essential to determine whether the stress proteins involved (Hsp70, Caspase-3 and Rad54) are Raman active and to identify their corresponding characteristic Raman bands and therefore 3-D silver colloidal nanosphere synthesis procedure was opted. We were able to detect successfully the standard form of all three stress proteins utilizing non-specific detection by SERS. Specifically, we were able to detect 1 ng/ml of Caspase-3 proteins, below the level of detection (4.8 ng/ml) in ELISA. To advance the application the biocompatibility of silver nanoparticles in the yeast cells will be investigated as an alternative to gold.

5.3.1. Future Plan

- Measure standard forms of Caspase-3, Rad54 and Hsp70 proteins using antibody-tagged Gold Nanoparticles. If not successful, Raman-labeling the Gold Nanoparticles to detect proteins indirectly will be attempted
- Demonstrate uptake of Gold Nanoparticle conjugate by yeast cells and evaluation of 3-D Silver colloidal nanosphere for the bio-compatibility in the yeast cells
- Exposure of live yeast to environmental stresses after the uptake of the SERS sensors to detect the stress response directly from the yeast.
- Design and test a platform for storage of live yeast loaded with the SERS sensors.

5.4. General Conclusion

Currently there is no practical or rapid method to monitor exposure to genotoxic agents of unknown nature. The current approach for assessing genome toxicity relies principally on scoring chromosomal abnormalities. These measures of genotoxicity are currently only possible through laborious cytogenetic evaluations requiring dedicated lab personnel with extensive training. We have made significant progress toward development of two prototype biosensors to detect non-specific DNA damage: (i) EIST biosensor measuring reactive oxygen species specifically 8-OHdG; and (ii) SERS biosensor measuring several stress proteins. In addition, we are in the process of validating the cytogenetic assays necessary. We are well on our way towards achieving the benchmarks expected for the first year of this project.

These three seemingly disparate projects detailed in this report will culminate in a common goal to compare the sensitivity and specificity of the ability of these two prototype biosensors to detect

genotoxic damage, as determined by gold-standard cytogenetic assays. Success of one or both of the biosensor devices compared to that of standard genotoxic assays will be established using standard statistical methodology, and judged by the ability of the devices to achieve equal or increased sensitivity of the gold-standard assays. Specifically, do the biosensors produce a measurable response at the same genotoxic concentration as in cytogenetic assays, and do the biosensor devices produce a dose related response as seen in the cytogenetic assays? We will then be able to determine whether one or more biosensor has the ability to detect the presence of toxicants more rapidly and sensitively than conventional cytogenetics assays. If so, we will then focus future efforts toward assuring "rugged" devices suitable to be worn or utilized in military theatre. This will require experimentation in collaboration with TATRC beyond the current time span of this contract.

6. References

Aroca R. Surface-Enhanced Vibrational Spectroscopy, John Wiley & Sons Ltd., Chichester, England, 2006

Bai F., Wang D., Huo Z., Chen W., Liu L., Lian X., Chen C., Wang X., Peng Q.A., Li Y. "A Versatile Bottom-up Assembly Approach to colloidal Spheres from Nanocrystals", Angew. Chem. Int. Ed. 46, 6650-6653, 2007.

Erhola, M., Toyokuni, S., Okada, K., Tanaka T., Hiai, H., Ochi, H., Uchida, K., Osawa, T., Nieminen, M.M., Alho, H. and Kellokumpu-Lehtinen, P., "Biomarker evidence of DNA oxidation in lung cancer patients: association of urinary 8-hydroxy-2'-deoxyguanosine excretion with radiotherapy, chemotherapy, and response to treatment.", FEBS Lett. 409, 287-291, 1997

Glei M., Hovhannisvan G., Pool-Zobel B.L. "Use of Comet-FISH in the Study of DNA Damage and Repair: Review". Mutat. Res. 681, 33-43, 2009.

Glover T.W., Stein C.K. "Chromosome Breakage and Recombination at Fragile Sites". Am. J. Hum. Genet. 43, 265-273, 1988.

Gordillo M., Vega H., Jabs E.W. " Roberts Syndrome" Gene Reviews 1993-2009.

Kang, K.A., Zhang, R., Lee, K.H., Chae, S., Kim, B.J., Kwak, Y.S., Park, J.W., Lee, N.H., and Hyun, J.W. "Protective effect of triphlorethol-A from Ecklonia cava against ionizing radiation in vitro", J. Radiat. Res., 47, 61–8, 2006.

Kasai, H.; Nishimura, S. "Hydroxylation of deoxyguanosine at the C-8 position by ascorbic acid and other reducing agents", Nucleic Acids Res., 12, 2137-2145, 1984.

Katz, E., "Application of bifunctional reagents for immobilization of proteins on a carbon electrode surface: Oriented immobilization of photosynthetic reaction centers", J. Electroanal. Chem., 365, 157-164, 1994.

Kim D., Heo J., Kim M., Lee Y. W., Han S.W. “Size-controlled synthesis of monodisperse gold nanooctahedrons and their surface-enhanced Raman scattering properties”. J. Chem. Phy. Letters. 468, 245-248, 2009.

Kim D.Y., Li W., Ma Y., Yu T., Li Z., Park O., Xia Y. “Seed-Mediated Synthesis of Gold Octahedra in High Purity and with Well-Controlled Sizes and Optical Properties”. Chem. Eur. J. 17, 4759-4764, 2011.

Kuhn, J.F., Hoerth, P., Hoehn, S.T., Preckel, T., and Tomer, K.B. “Proteomics study of anthrax lethal toxin-treated murine macrophages”. Electrophoresis. 27, 1584–97, 2006.

Li, H., J Sun, B.M. Cullum. “Label-free detection of proteins using SERS-based immune- nanosensors”. NanoBiotechnology. DOI: 10.1385/Nano:2:1-2:17, 2006

Li, C-Z., Vandernberg, K., Prabhulkar, S., Zhu, X., Schneper, L., Mathee, K., Rosser, C.J., Almeide, E., “Paper based point-of-care testing disc for multiplex whole cell bacteria analysis”. Biosensors and Bioelectroncs, 26, 4342-4348, 2011.

Mager, W.H., Ferreira, P.M. “Stress response of yeast”. Biochem J. 290:1-13, 1993.

Ngom, B., Guo, Y., Wang, X., Bi, D. "Development and application of lateral flow test strip technology for detection of infectious agents and chemical contaminants: a review". Anal Bioanal Chem., 397, 1113-1135, 2010.

Nie, Shuming and Emory, Steven. “Probing Single Molecules and Single Nanoparticles by Surface-Enhanced Raman Scattering”. Science 21 February 1997: Vol. 275 no. 5303 pp. 1102-1106 DOI: 10.1126/Science.275.5303.1102

Sari-Minodier I., Orsiere T., Auquier P., Martin F., Botta A. “Cytogenetic Monitoring By Use Of The Micronucleus Assay Among Hospital Workers Exposed To Low Doses Of Ionizing Radiation”. Mutat. Res. 618, 111-121, 2007.

Sperati A, Abeni DD, Tagesson C, Forastiere F, Miceli M, Axelson O., “Exposure to indoor background radiation and urinary concentrations of 8-hydroxydeoxyguanosine, a marker of oxidative DNA damage”. Environ. Health Perspect. 107, 213–215, 1999.

Wang D., Li Y. “Effective Octadecylamine System for Nanocrystal Synthesis”. Inorg. Chem. 40, 5196-5202, 2011.

Wang D., Xie T., Peng Q., Li Y. “Ag, Ag_2S, and Ag_2Se Nanocrystals: Synthesis, Assembly, and Construction of Mesoporous Structures”. J. Am. Chem. Soc. 130, 4016-4022, 2008.